The FEBS Journal

FEBS PRESS science publishing by scientists

The common marmoset as suitable nonhuman alternative for the analysis of primate cochlear development

Makoto Hosoya[1], Masato Fujioka[1], Ayako Y. Murayama[2,3], Hideyuki Okano[2,3] and Kaoru Ogawa[1]

1 Department of Otorhinolaryngology, Head and Neck Surgery, Keio University School of Medicine, Tokyo, Japan
2 Department of Physiology, Keio University School of Medicine, Tokyo, Japan
3 Laboratory for Marmoset Neural Architecture, Center for Brain Science, RIKEN, Wako, Japan

Keywords
cochlea; common marmoset; inner ear; primate

Correspondence
M. Fujioka, Department of Otorhinolaryngology, Head and Neck Surgery, Keio University School of Medicine, 35 Shinanomachi, Shinjuku-ku, Tokyo 160-8582, Japan
Tel: +81 3 5363 3827
E-mail: masato@2002.jukuin.keio.ac.jp

(Received 14 November 2019, revised 30 January 2020, accepted 20 April 2020)

doi:10.1111/febs.15341

Cochlear development is a complex process with precise spatiotemporal patterns. A detailed understanding of this process is important for studies of congenital hearing loss and regenerative medicine. However, much of our understanding of cochlear development is based on rodent models. Animal models that bridge the gap between humans and rodents are needed. In this study, we investigated the development of hearing organs in a small New World monkey species, the common marmoset (*Callithrix jacchus*). We describe the general stages of cochlear development in comparison with those of humans and mice. Moreover, we examined more than 25 proteins involved in cochlear development and found that expression patterns were generally conserved between rodents and primates. However, several proteins involved in supporting cell processes and neuronal development exhibited interspecific expression differences. Human fetal samples for studies of primate-specific cochlear development are extremely rare, especially for late developmental stages. Our results support the use of the common marmoset as an effective alternative for analyses of primate cochlear development.

Introduction

Auditory perception is the process by which mechanical sound waves are detected by the inner ear and converted into neuronal electrical impulses that are perceived by the brain. The inner ear is the peripheral sensory organ for hearing and equilibrium. In mammals, the inner ear can be divided into two parts, the cochlea for the sense of hearing and the vestibule/semicircular canal for the sense of equilibrium. In the cochlea, hair cells convert mechanosensory sound waves into neural electrical pulses.

The cochlea is a mammal-specific hearing organ. Other vertebrates have comparable sensory organs for auditory perception, consisting of mechanosensory hair cells arranged in discrete sensory patches for the transduction of various mechanical stimuli (sound and gravity or tilt) [1]. Fishes use an otolith [2], which is the most primitive organ for sound perception. Amphibians [3], reptiles [4,5], and birds use the basilar papilla [6]. The evolutionary acquisition of the cochlea is recent; thus, there is variation in cochlear

Abbreviations
AQP4, aquaporin 4; ATP1A1, ATPase Na+/K+ transporting subunit alpha 1; CALB1, calbindin; CALB2, calbindin2; CALD1, caldesmon 1; CDKN1B, cyclin-dependent kinase inhibitor 1B; FGFR3, fibroblast growth factor receptor 3; GATA3, GATA binding protein 3; GER, greater epithelial ridge; ISLET1, ISL LIM homeobox 1; LER, lesser epithelial ridge; MLANA, Melan A; MYO7A, myosin VIIA; NEFH, neurofilament heavy; NKCC1, Na-K-Cl cotransporter 1; PCNA, proliferating cell nuclear antigen; POU3F4, POU class 3 homeobox 4; POU4F3, POU class 4 homeobox 3; PRPH, peripherin; PVALB, parvalbumin; SLC26A5, solute carrier family 26 member 5; SOX10, SRY-box transcription factor 10; SOX2, SRY-box transcription factor 2; SOX21, SRY-box transcription factor 21; SOX9, SRY-box transcription factor 9; TBX18, T-box transcription factor 18; TUBB, tubulin beta.

morphology, even among mammals [7-9]. For example, the cochlea of monotremes is relatively short and curved (without a complete full coil) [10,11] with multiple rows of inner hair cells and pillar cells [10]. Therians have relatively long and fully coiled cochlea with a single row of inner hair cells and two rows of pillar cells [12-14].

The development of the cochlea requires multiple fine-tuned steps [15-18]. The process starts with the formation of the otic placode in the ectoderm, followed by neural tube formation. The otic vesicle then forms from the otic placode and becomes the inner ear, including the cochlea and vestibule/semicircular canal. At the time of cochlear duct formation, the maturation of the sensory epithelium occurs, along with hair cell and supporting cell differentiation. During the formation of the cochlea and vestibule, bidirectional neural innervation occurs between the inner ear and brain.

Our understanding of cochlear development is largely based on studies of rodent models [19,20]. The mouse model is useful for understanding basic human cochlear development, developing therapeutic agents for hearing loss, and realizing regenerative therapy. However, several issues limit the application of rodent models to humans. Some mouse models fail to reproduce human congenital hearing loss [20], indicating that the factors involved in cochlear development differ between rodents and humans.

Human cochlear development and congenital malformation are not fully explained by a rodent model. Evolutionarily, the cochlea was acquired relatively recently and exhibits differences among species [9,11-12,14,21]. Therefore, analyses of human fetal samples are important for understanding cochlear development. However, these studies are limited by ethical issues and rare access to human fetal samples. It is extremely difficult to obtain well-prepared human fetal samples suitable for molecular biological analyses (especially for the late stage of cochlear development, after 16 weeks of gestation).

Therefore, a nonhuman primate model, more closely related to humans than are rodents, is necessary for investigating the development of hearing organs. A small New World monkey species, the common marmoset (*Callithrix jacchus*), has been used for vocal communication and audiological research [22-27]. Recently, the species has been used for hereditary hearing loss research [28-33]. Moreover, genetic modification is now possible in the common marmoset [34-36].

In this study, we investigated the cochlea of embryos and neonates of the common marmoset and compared them with those of mouse and human reported previously. We provide a detailed description of the morphogenesis of the sensory epithelium (including the organ of Corti and hair cells), spiral ganglion neurons, lateral wall fibrocytes, and stria vascularis. We found that cochlear development is completed at birth in both the common marmoset and humans but continues to neonatal P14 in mice. The duration of cochlear development in the common marmoset is longer than that in rodents and is very similar to that in humans. Moreover, we examined the expression patterns of more than 25 proteins in the inner ear, all of which are established developmental markers of inner ear cells or important factors in cochlear development. Some proteins had spatiotemporally distinct expression patterns between primates and rodents.

Results and Discussion

Morphological analysis of the developing cochlea in the common marmoset

We first examined morphological changes of the cochlea during development in the common marmoset

Fig. 1. Histological analysis of the developing cochlea in the common marmoset by hematoxylin–eosin staining. (A) Schematic diagram comparing cochlear development between species. (B–E) A cross-sectional view of the common marmoset cochlea duct in a E96 embryo. At E96, cochlear duct formation was complete, while the formation of the scala vestibule (* in B and C) and scala tympani (** in B and C) started from the basal turn and was not observed in the apical turn and middle turn. Arrowheads in C indicate developing Reissner's membrane. (F–I) A cross-sectional view of the common marmoset cochlea duct in a E101 embryo. At E101, the spaces of the scala vestibuli (* in F) and the scala tympani (** in F) could be observed through all turns. In this stage, the organ of Corti was not developed. (J–M) A cross-sectional view of the common marmoset cochlea duct in a E115 embryo. At E115, the overall cochlear duct was well-developed. The scala vestibuli and the scala tympani were fully formed. In the scala media, sensory epithelial formation was still immature, and organ of Corti and stria vascularis formation was incomplete. (N–Q) A cross-sectional view of the common marmoset cochlea duct in a P0 neonate. At P0, the scala media was fully developed and the organ of Corti was mature, with a well-formed tunnel of Corti. The stria vascularis was composed of three layers: marginal cells (black arrow), intermediate cells (white asterisk), and basal cells (white arrow) in Q. Higher magnification image of cochlear duct (C, G, K, and O), sensory epithelium or organ of Corti (D, H, L, and P) and stria vascularis (E, I, M, and Q) in basal turns at each stage are shown. Scale bar: 200 μm in B, F, J, and N, 50 μm in C–E, G–I, K–M, P and Q. E96 (n = 5), E101 (n = 4), E115 (n = 4), and P0 (n = 3).

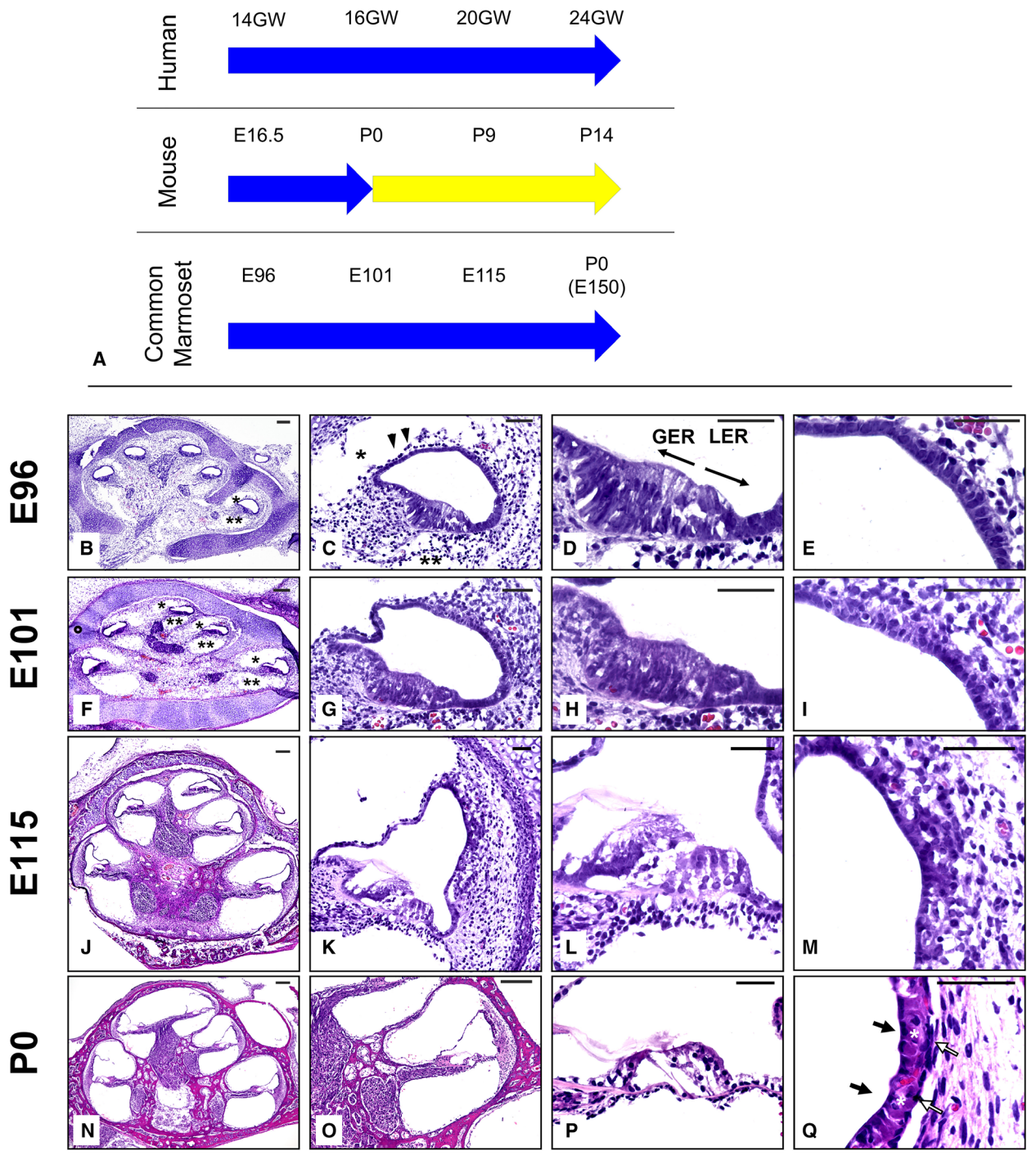

by hematoxylin–eosin staining (Fig. 1). In fetal cochlear development, the differentiation of auditory hair cells begins at 12–14 weeks of gestation in humans [37,38] and at around E16.5 in mice. We detected the differentiation of auditory hair cells at around E96 in the common marmoset fetus (Fig. 1A).

The common marmoset has a gestation period of about 150 days [39]. In E96 embryos of the common marmoset, cochlear duct formation was complete and three turns (apical turn, middle turn, and basal turn) were observed (Fig. 1B). However, the formation of the scala vestibule and scala tympani was incomplete.

We observed their formation from the basal turn, but not from the apical turn or middle turn. In the basal turn, Reissner's membrane began to form (Fig. 1C). Histologically, the greater epithelial ridge (GER) and the lesser epithelial ridge (LER) could not be distinguished at the apical turn, in which the epithelial cells were still homogeneously thick, but were detected at the middle turn and the basal turn (Fig. 1D).

In the human fetal cochlea, the anatomical maturation of the scala tympani and scala vestibuli occurs at around 15–16 weeks of gestation [38,40]. At E101 of the common marmoset, we observed the spaces of the scala vestibuli and the scala tympani from the basal turn to the apical turn, but development was incomplete (Fig. 1F,G). We observed the GER and LER at the apical turn as well as in the middle turn and basal turn. At this stage, the organ of Corti was still not completely developed (Fig. 1H).

In E115 embryos of the common marmoset, the cochlear duct was well-developed (Fig. 1J,K). The scala vestibuli and the scala tympani were fully developed. Notably, at this stage, we observed the crescent form of the lateral wall fibrocytes. In the scala media, the sensory epithelium formation was still immature. The organ of Corti and stria vascularis formation was not complete (Fig. 1K,L). On the LER side, outer sulcus cells, Claudius cells, and Hensen's cells were well-formed at this stage (Fig. 1K). However, on the GER side, the cells within Kölliker's organ were not regressed, and inner sulcus cells did not form a monolayer. In the organ of Corti, the tunnel of Corti began to form (Fig. 1L).

At postnatal day 0 (equivalent to about 150 days of gestation [39]), cochlear formation was complete (Fig. 1N), including development of the scala media, organ of Corti, and tunnel of Corti (Fig. 1P). The stria vascularis comprised three layers, marginal cells, intermediate cells, and basal cells (Fig. 1Q).

Development of hair cells

We evaluated hair cells by examining the expression of several markers, including POU4F3 (POU class 4 homeobox 3, Brn3c) [41] as an early development marker and MYO7A (myosin VIIA) [42] and CALB1 (calbindin 1) [43] as late development markers. We also evaluated the expression of SLC26A5 (solute carrier family 26 member 5, prestin) [44] as a specific marker of outer hair cells. Moreover, we used CALB2 (calbindin 2, calretinin) [45] and PVALB (parvalbumin) [46] as specific markers of inner hair cells.

POU4F3 is a POU domain factor that is crucial for inner ear hair cell development. Targeted null *Pou4f3* mutants have no mature hair cells [41], and mutations in *POU4F3* cause nonsyndromic hearing loss in humans (DFNA15) [47]. In mouse, hair cells of the cochlear sensory epithelia initiate Pou4f3 expression as early as E14.5 [48,49].

MYO7A is a member of the myosin facility of proteins, which function as mechanoenzymes by hydrolyzing ATP to move along actin filaments. The shaker-1 mouse mutant with a mutation in *Myo7a* shows abnormal sensory hair development [50,51]. In human, a mutation of *MYO7A* is responsible for Usher syndrome type 1B [52], as well as nonsyndromic deafness [53]. In mice, Myosin7a-positive cells are first detected in auditory hair cells at E16 [54], which is 1 day later than Pou4f3 expression [48].

In humans, hair cell development starts between 12 and 14 weeks of gestation [38]. At 14 weeks of gestation, only one row of inner hair cells is present in the apical turn, while in the basal turn, one row of inner hair cells and three rows of outer hair cells are present. At E96 of the common marmoset fetus, hair cell development differed between turns (Fig. 2A–C), similar to humans at 14 weeks of gestation [38]. In the apical turn, we detected a single row of POU4F3-positive and MYO7A-negative cells medial to the sensory epithelial region marked by SOX2 immunostaining (Fig. 2A). POU4F3-positive cells were likely immature inner hair cells. In the middle turn, we observed outer and inner hair cells as three lateral rows and one medial row. Both outer hair cells and inner hair cells were observed as POU4F3-positive and MYO7A-positive cells in the sensory epithelial region (Fig. 2B). MYO7A immunoreactivity was strong in inner hair

Fig. 2. Hair cell development in the common marmoset. (A–C) At E96, POU4F3 and MYO7A were expressed in middle and basal turns but only a low of inner hair cells showed POU4F3 expression in the apical turn (arrow in A). SOX2 was expressed broadly in the prosensory domain. (D, E) POU4F3 and MYO7A were expressed in hair cells at E101 and E115. In E101, SOX2 expression was observed broadly in prosensory domain including hair cells. In E115, SOX2 expression was observed in Hensen's cells, Deiters' cells, inner and outer pillar cells, inner border cells, inner pharyngeal cells, and inner sulcus cells. (F) MYO7A expression was observed in hair cells, but no POU4F3 expression was detected in the cochlea at P0. At P0, SOX2 expression was observed in Hensen's cells, Deiters' cells, inner and outer pillar cells, inner border cells, and inner pharyngeal cells. The nuclei were counterstained with Hoechst (blue). Scale bar: 50 μm. D–F: basal turn. IHC, inner hair cells; OHC, outer hair cells. E96 (n = 5), E101 (n = 4), E115 (n = 4), and P0 (n = 3).

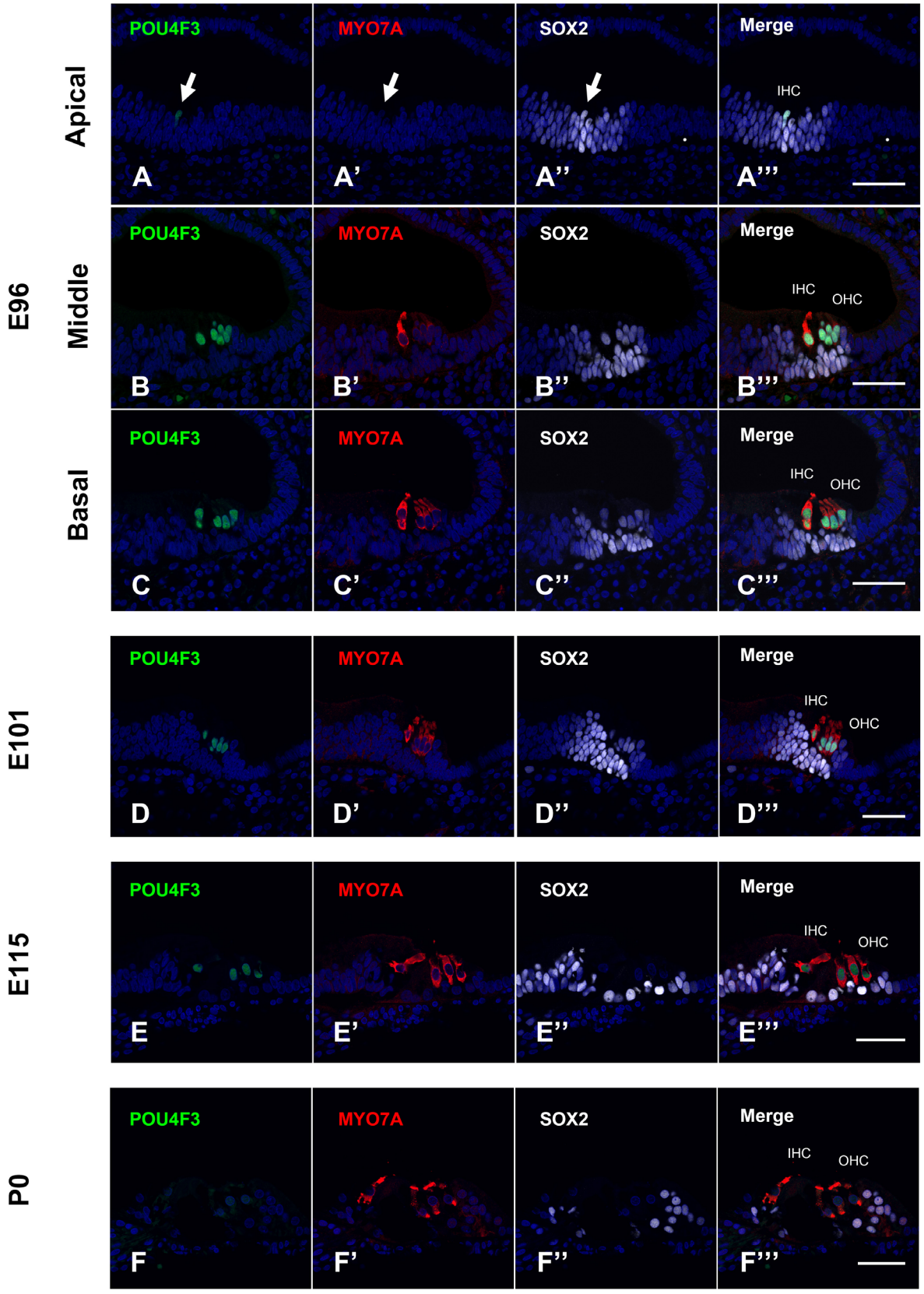
E96
E101
E115
P0
Apical
Middle
Basal
POU4F3
MYO7A
SOX2
Merge
IHC
OHC
A
A'
A''
A'''
B
B'
B''
B'''
C
C'
C''
C'''
D
D'
D''
D'''
E
E'
E''
E'''
F
F'
F''
F'''

cells (Fig. 2B'). In the basal turn, one row of inner hair cells and three rows of outer hair cells were observed as POU4F3-positive and MYO7A-positive cells (Fig. 2C). These findings indicated that inner hair cell development was followed by outer hair cell development with progression from the basal to apical turns in the common marmoset, consistent with the progression in rodents and humans. Notably, at this stage, all POU4F3-positive cells showed SOX2 expression (Fig. 2A–C, arrow in A). At E101, there was no difference among turns with respect to hair cell marker expressions. Three rows of outer hair cells and one row of inner hair cells were POU4F3-positive and MYO7A-positive (Fig. 2D). Hair cell differentiation extended all the way to the apex between E96 and E101. Slight SOX2 expression was detected in both outer and inner hair cells (Fig. 2D"). At E115, the three rows of outer hair cells and one row of inner hair cells were POU4F3-positive, MYO7A-positive, and SOX2-negative (Fig. 2E). Corti tunnel formation was apparent between these hair cells. At P0, POU4F3 expression was absent from outer hair cells and inner hair cells (Fig. 2F). The subcellular expression pattern of MYO7a changed between E115 and P0. Cytoplasmic MYO7A expression decreased and exhibited a membranous pattern, in which relatively high expression of MYO7a was detected in stereocilia, the cuticular plate, and bottom of the hair cell body (Fig. 2F').

CALB1, a calcium-binding protein, is expressed in the inner ear. Calcium-binding proteins are involved in the regulation of mechanoelectrical transduction mechanisms and in the afferent synaptic neurotransmitter release in the inner ear. In mouse, CALB1-positive cells are first detected in cochlear inner hair cells at E16 and outer hair cells at E18 [43]. In the common marmoset, we only detected CALB1 expression in the inner hair cells of basal turns at E96 (Fig. 3A). At E101, E115, and P0, CALB1 expression was detected in the outer hair cells and inner hair cells of all turns (Figs 3B–D and 4).

In this study, we used SLC26A5, a transmembrane motor protein specifically localized to the outer hair cells of the mammalian inner ear, as an outer hair cell marker. Voltage-dependent conformational changes in SLC26A5 are thought to generate changes in the length of the outer hair cell. In mice, Slc26a5 expression begins at P4–P5 and is maximal by P10 [55]. In the common marmoset, SLC26A5 expression was not detected until E101 (Fig. 3I). At E115, weak SLC26A5 expression was detected only in outer hair cells (Fig. 3J). At P0, strong SLC26A5 expression was detected only in outer hair cells (Figs 3K and 4).

PVALB and CALB2 were used as inner hair cell markers. Like CALB1, PVALB is another calcium-binding protein. In mouse, PVALB expression begins in inner and outer hair cells at P3 and starts to decrease in outer hair cells by P8 [56,57], after which its expression is restricted to inner hair cells. In mouse, the expression of CALB2, another calcium-binding protein, begins in inner hair cells at P0 and in outer hair cells at P2 and starts to disappear from outer hair cells at P9-10. In adult mouse, its expression is only detected in inner hair cells [45]. In the common marmoset, PVALB expression was only detected in inner hair cells at E96 (Fig. 3E). At E101, PVALB expression was detected in both outer hair cells and inner hair cells (Fig. 3F), while CALB2 expression was not detected (Fig. 3L). At E115, PVALB and CALB2 were observed in both hair cell types, although their expression in outer hair cells was lower at P0 (Figs 3G,H,M, N and 4). At around E115, the differences in expression patterns of SLC26A5, PVALB, and CALB2 became more obvious between inner and outer hair cells.

Expression of supporting cell markers

We investigated the development of supporting cells by immunostaining for several markers, including SOX2 (SRY-box transcription factor 2), CDKN1B (cyclin-dependent kinase inhibitor 1B, p27kip1),

Fig. 3. Expression of conventional hair cell markers in the developing cochlea of the common marmoset. (A) At E96, CALB1 expression was detected only in the inner hair cells of basal turns. (B, C) At E101 and E115, CALB1 expression was detected in three rows of outer hair cells and one row of inner hair cells. (D) At P0, CALB1 expression was mainly detected in inner hair cells with slight expression in outer hair cells. (E) At E96, PVALB expression was only detected in the inner hair cells. (F, G) At E101 and E115, PVALB expression was detected in both outer hair cells and inner hair cells. (H) At P0, PVALB expression was mainly detected in inner hair cells with slight expression in outer hair cells. (I) SLC26A5 expression was not observed at E101. (J) Slight SLC26A5 expression was detected at E115. (K) At P0, strong SLC26A5 expression was observed in outer hair cells. (L) At E101, CALB2 expression was not detected in outer hair cells or inner hair cells. (M, N) At E115 and P0, CALB2 expression was detected in both outer hair cells and inner hair cells. The nuclei were counterstained with Hoechst (blue). Scale bar: 50 μm. A–C, E, F, H, I–K, N: basal turn; D and L: middle turn; G: apical turn. IHC, inner hair cells; OHC, outer hair cells. E96 (n = 5), E101 (n = 4), E115 (n = 4), and P0 (n = 3).

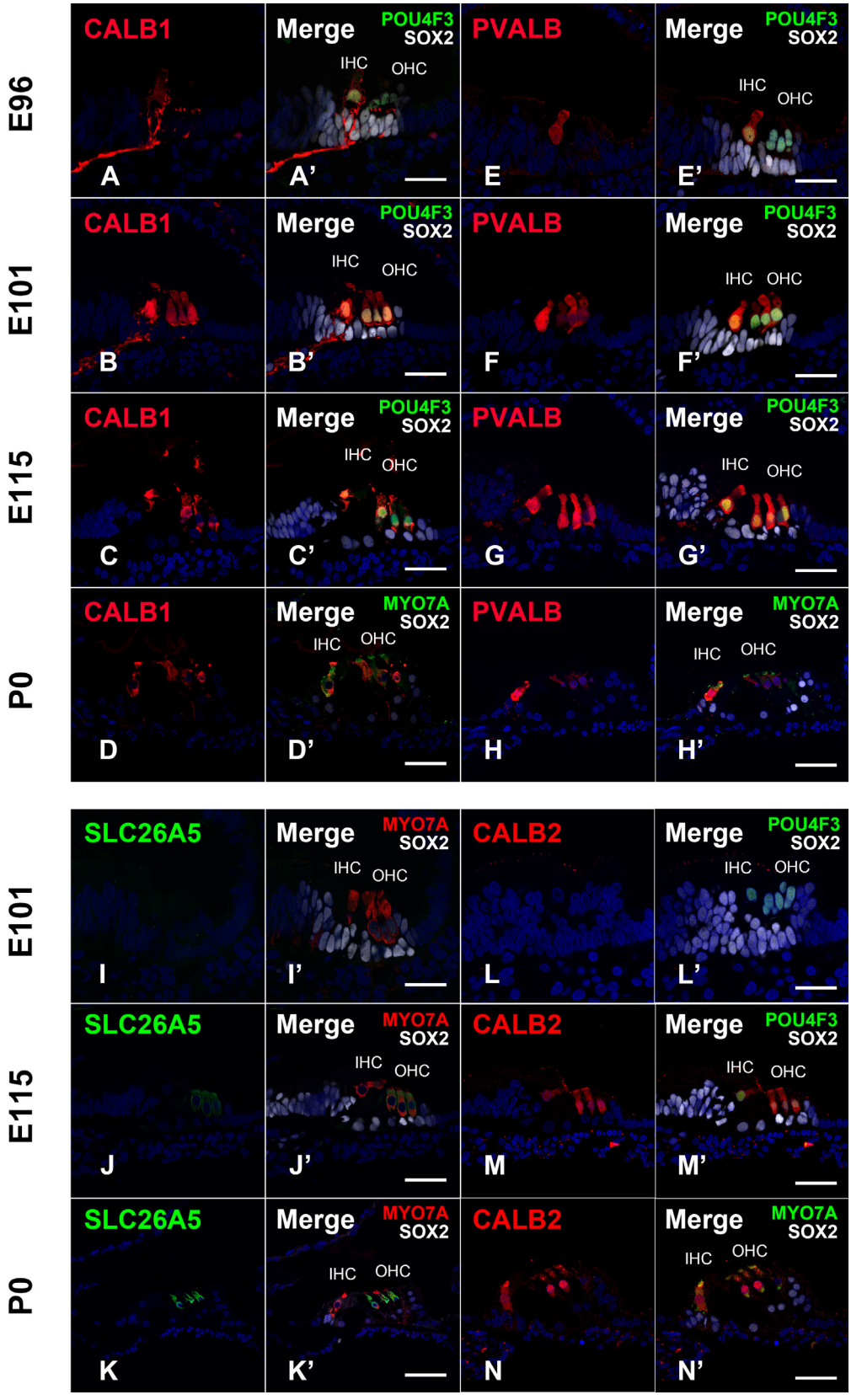
E96
E101
E115
P0
E101
E115
P0
CALB1
Merge
POU4F3
SOX2
MYO7A
PVALB
CALB2
SLC26A5
IHC
OHC
A
A'
B
B'
C
C'
D
D'
E
E'
F
F'
G
G'
H
H'
I
I'
J
J'
K
K'
L
L'
M
M'
N
N'

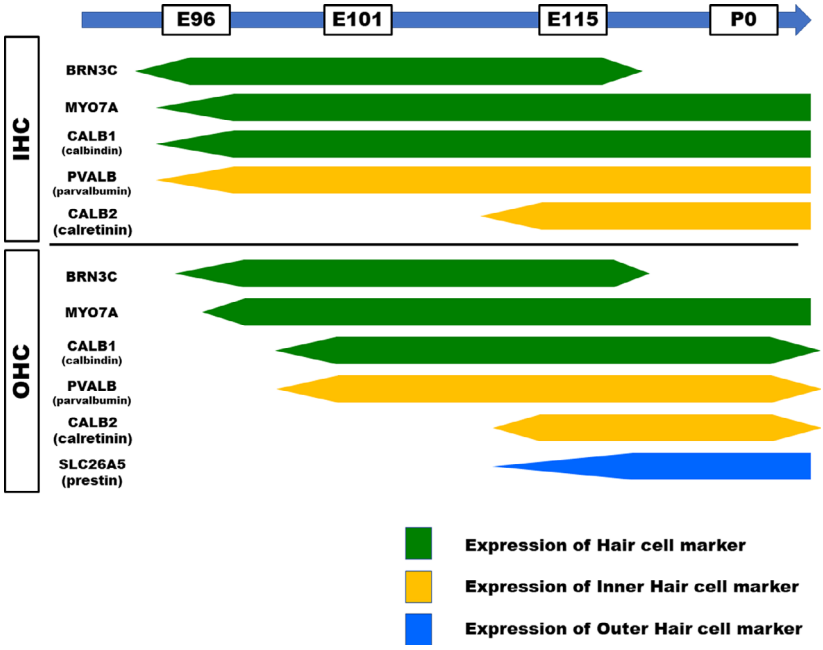

Fig. 4. Schematic diagram of conventional hair cell marker expression patterns. Changes in expression patterns of marker genes, known as both inner and outer hair cell markers, are indicated by green lines. Expression of inner hair cell-specific markers, which can only be observed in inner hair cells in adults, is indicated by yellow line. Expression of outer hair cell-specific markers, which can only be observed in outer hair cells in adults, is indicated by blue line. IHC, inner hair cells; OHC, outer hair cells.

GATA3 (GATA binding protein 3), ISLET1 (ISL LIM homeobox 1), FGFR3 (fibroblast growth factor receptor 3), AQP4 (aquaporin 4), and CD44 [58] (Fig. 5).

At E96, we detected SOX2 in the prosensory domain as PCNA (proliferating cell nuclear antigen)-negative regions of the cochlear duct, in which immature hair cells are included. SOX2 expression became more restricted over time (Figs 2A”–C” and 6). At this stage, we also detected expression in the spiral ganglion. As development progressed, we observed a decrease in SOX2 expression in hair cells and no expression in hair cells at E115 (Fig. 2D”,F”). We observed SOX2 expression in Hensen’s cells, Deiters’ cells, inner and outer pillar cells, inner border cells, inner pharyngeal cells, and inner sulcus cells at E115 (Fig. 2E”). At P0, we did not detect SOX2 in inner sulcus cells but still observed this marker in Hensen’s cells, Deiters’ cells, inner and outer pillar cells, inner border cells, and inner pharyngeal cells (Figs 2F” and 5).

CDKN1B, a cyclin-dependent kinase inhibitor, regulates quiescence and cell proliferation in hair cells and supporting cells in the inner ear [54,59] and is negatively correlated with regenerative potential in other tissues. Combining a *Cdkn1b* deletion with ectopic *Atoh1* expression leads to the conversion of supporting cells into hair cells in the mature mouse cochlea [60]. In mice, Cdkn1b is broadly expressed in supporting cells, including Hensen’s cells, Deiters’ cells, and inner and outer pillar cells, but it is not expressed in inner and outer hair cells at P0, and this pattern is maintained until the adult stage [59]. In the common marmoset cochlea, we only detected CDKN1B in SOX2-positive supporting cells and not in hair cells at E96 (Figs 6 and 7A). At E101, CDKN1B was expressed more broadly in supporting cells and was expressed more widely than SOX2 in the sensory epithelium (Fig. 6B). At E115, CDKN1B showed broad expression from outer sulcus cells to interdental cells (Fig. 7C). It was detected in supporting cells but not in hair cells at E101 and E115 (Fig. 7B,C), consistent with its expression in the mouse P0 cochlea. However, its expression was lost in most supporting cells, except in inner border cells and Hensen’s cells, at birth (Figs 5 and 7D).

ISLET1 is a LIM-homeodomain transcription factor. The overexpression of *Islet1* can promote hair cell survival and thereby minimize hearing impairment in mice. Thus, *ISLET1* is a therapeutic target for hearing loss in humans [61]. In mice, Islet1 is expressed in the prosensory region of otocysts, young hair cells, and supporting cells at E13.5, but it is restricted to spiral ganglion neurons and is no longer detected in the sensory domain after E16.5 [62]. In the common marmoset, we detected broad ISLET1 expression in the cochlear duct at E96 with relatively high expression in the ventral half (Fig. 7E). At E101, ISLET1 expression was restricted to the ventral half of the cochlear duct, including the GER and LER (Fig. 7F). We detected notably strong expression in inner hair cells and outer hair cells. At E115, we detected ISLET1 expression

Fig. 5. Schematic diagram of conventional supporting cell marker expression patterns. Changes in expression patterns of supporting cell markers are summarized. Expression in supporting cells was indicated in green, and expression in hair cells was indicated in yellow. Light colors indicate that only relatively weak expressions were observed. Stripes indicate that gene expression was observed in some cells of the cell population. IHC, inner hair cells; OHC, outer hair cells; ISC, inner sulcus cells; IBC, inner border cells; IPhC, inner pharyngeal cells; IPC, inner pillar cells; OPC, outer pillar cells; OSC, outer sulcus cells.

between the outer sulcus cells and inner sulcus cells (Fig. 7G). At P0, we observed ISLET1 in the outer sulcus cells, Claudius cells, Hensen's cells, Deiters' cells, outer pillar cells, inner pharyngeal cells, inner border cells, inner sulcus cells, and inner and outer hair cells (Figs 5 and 7H).

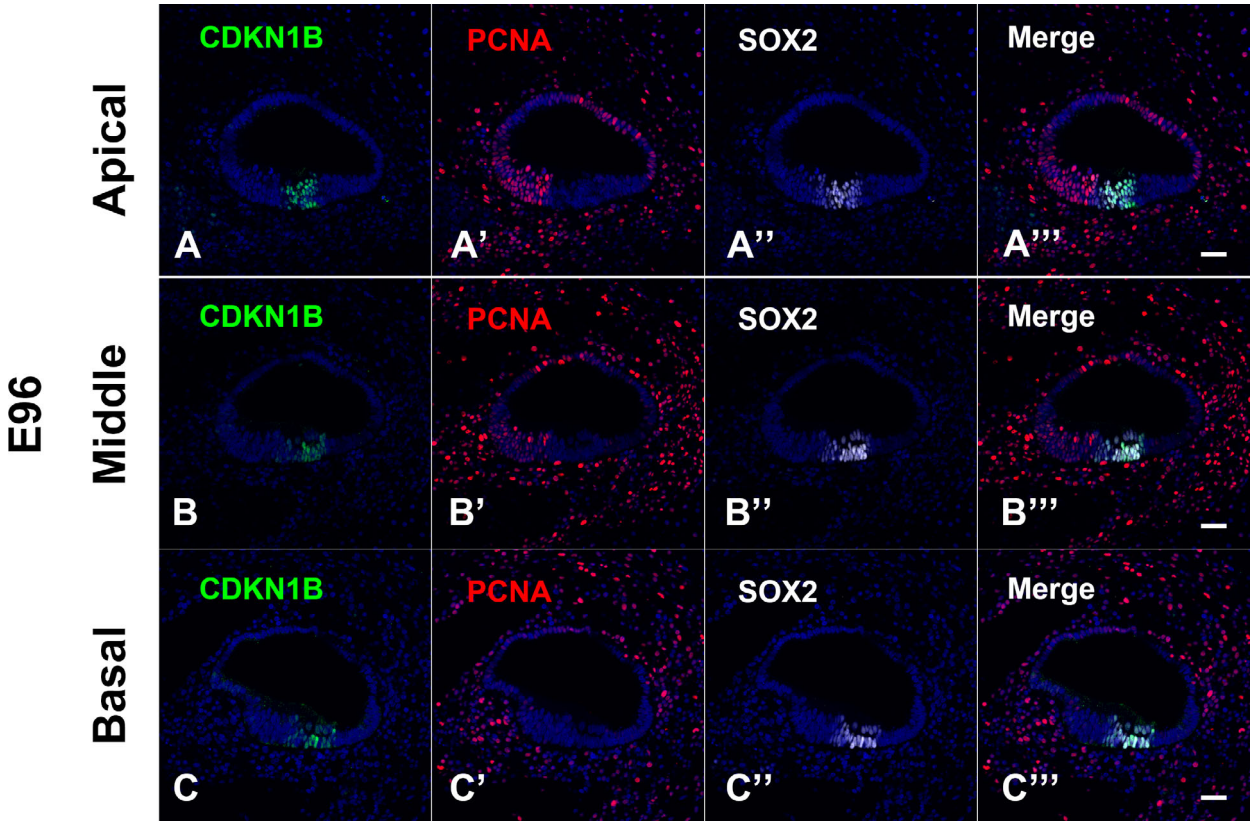

Fig. 6. Expression of prosensory epithelium markers in the common marmoset cochlea at E96. (A–C) In the common marmoset cochlea, CDKN1B expression was detected in PCNA-negative, SOX2-positive supporting cells but not in hair cells at E96. The nuclei were counterstained with Hoechst (blue). Scale bar: 50 μm. E96 (n = 5).

GATA3 has important roles in the regeneration and aging of hair cells [60]. In mice, at E18.5, Gata3 is highly expressed in all supporting cells and weakly expressed in hair cells [63]. After birth, Gata3 expression is largely lost from pillar cells and Deiters' cells but remains detectable in inner pharyngeal cells, inner border cells, Hensen's cells, and Claudius cells [60]. In the common marmoset, we detected GATA3

Fig. 7. Developmental changes in the expression patterns of CDKN1B, SOX2, ISLET1, and GATA3. (A) At E96, SOX2 was detected in the prosensory domain, including hair cells. Its expression became more restricted during cochlear development. At this stage, it was also observed in the spiral ganglion. CDKN1B was detected in only SOX2-positive supporting cells and was not detected in hair cells at E96. (B) At E101, CDKN1B was broadly expressed in the sensory epithelium. (C) At E115, SOX2 expression was observed in Hensen's cells, Deiters' cells, inner and outer pillar cells, inner border cells, inner pharyngeal cells, and inner sulcus cells. CDKN1B showed broad expression between the outer sulcus cells and interdental cells but was not detected in hair cells. (D) At P0, no SOX2 expression was detected in inner sulcus cells, but it was still observed in Hensen's cells, Deiters' cells, inner and outer pillar cells, inner border cells, and inner pharyngeal cells. CDKN1B expression was lost from most supporting cells, except for inner border cells and Hensen's cells at birth. (E) At E96, GATA3 was expressed on the lateral half of the cochlear duct, including in SOX2-positive cells other than hair cells. (F) At E101, GATA3 expression was restricted to the ventral side, including SOX2-positive cells other than hair cells. (G) At E115, GATA3 expression was observed between Claudius cells and interdental cells. Notably, at this stage, GATA3 expression was observed in outer and inner hair cells. (H) At P0, GATA3 exhibited relatively strong expression in Claudius cells, Hensen's cells, Deiters' cells, inner and outer pillar cells, inner hair cells, and inner sulcus cells, but relatively weak signals in outer hair cells, inner border cells, and inner pharyngeal cells. (I) At E96, ISLET1 was broadly expressed in the cochlear duct with relatively high expression in the ventral half. (J) At E101, ISLET1 expression was restricted to the ventral half of the cochlear duct, including GER and LER. Notably, strong expression was observed in inner hair cells and outer hair cells. (K) At E115, ISLET1 expression was detected between the outer sulcus cells and inner sulcus cells. (L) At P0, ISLET1 expression was observed in outer sulcus cells, Claudius cells, Hensen's cells, Deiters' cells, outer pillar cells, inner pharyngeal cells, inner border cells, inner sulcus cells, and inner and outer hair cells. The nuclei were counterstained with Hoechst (blue). Scale bar: 50 μm. A, B, E, F, I, and J: basal turn; C, D, G, K, and L: middle turn; H: apical turn. IHC: inner hair cells, OHC: outer hair cells. E96 (n = 5), E101 (n = 4), E115 (n = 4), and P0 (n = 3).

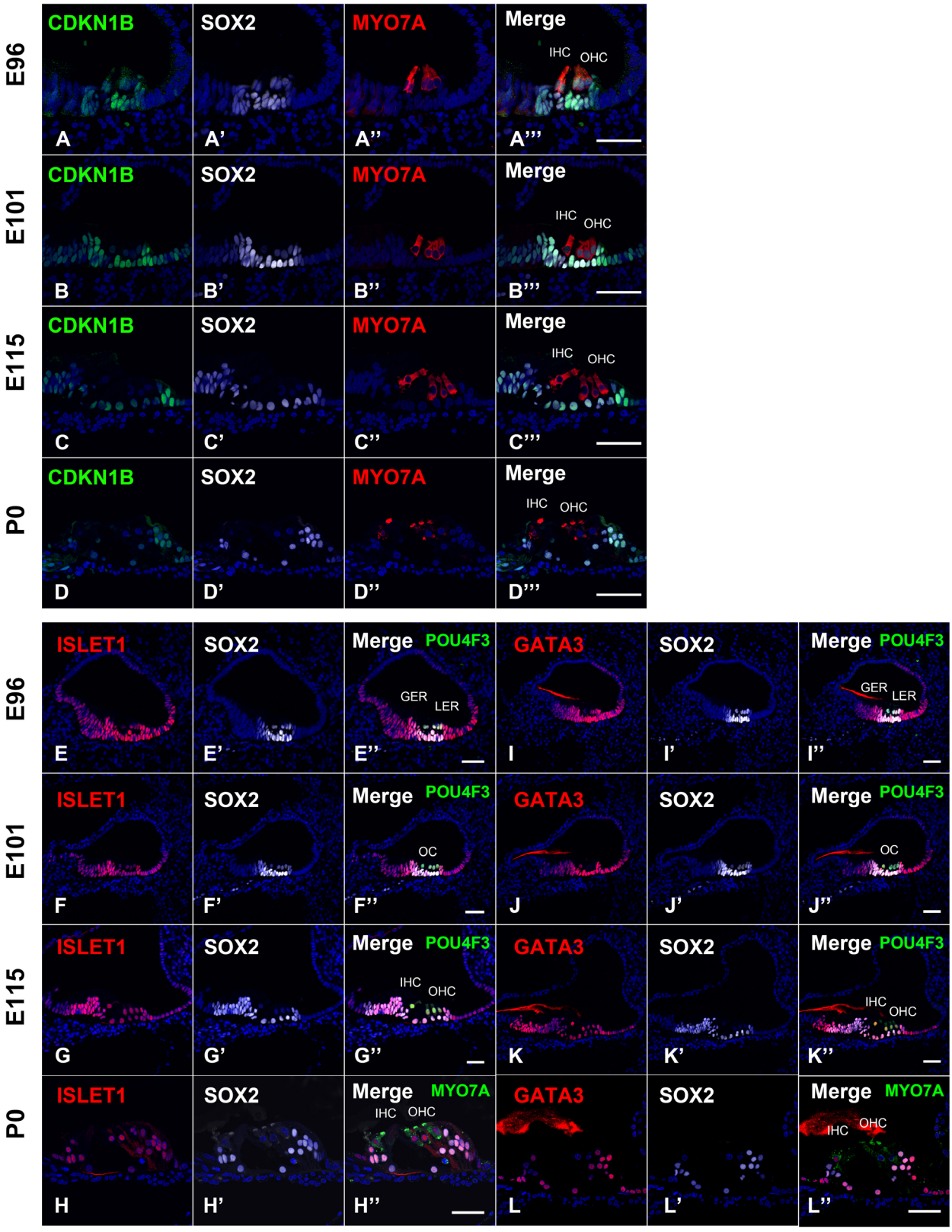
E96
E101
E115
P0
CDKN1B
SOX2
MYO7A
Merge
IHC
OHC
A
A'
A''
A'''
B
B'
B''
B'''
C
C'
C''
C'''
D
D'
D''
D'''
ISLET1
GATA3
POU4F3
GER
LER
OC
E
E'
E''
F
F'
F''
G
G'
G''
H
H'
H''
I
I'
I''
J
J'
J''
K
K'
K''
L
L'
L''

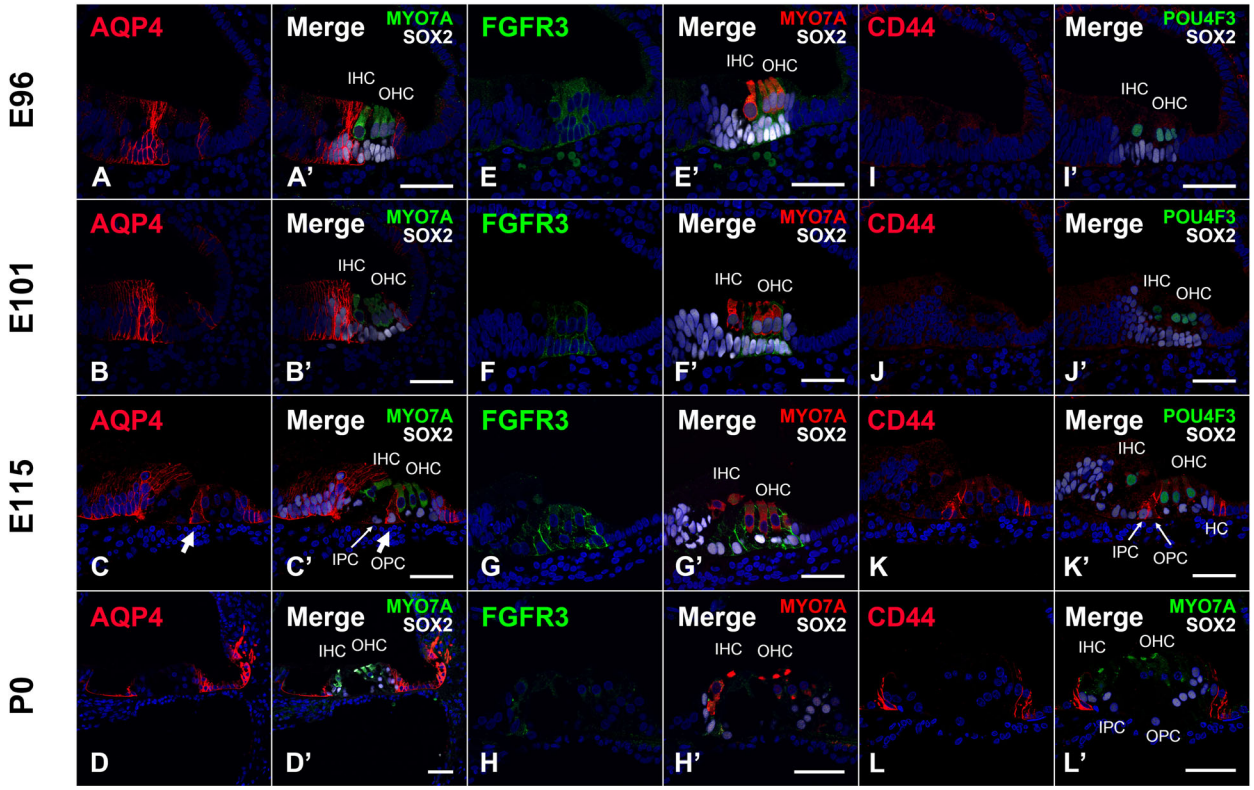

Fig. 8. Developmental changes in the expression patterns of AQP4, FGFR3, and CD44. (A) At E96, AQP4 was expressed at LER and GER but not in hair cells and substantial sensory epithelium between inner hair cells and outer hair cells. (B) At E101, AQP4 expression was detected in some supporting cells. (C) At E115, AQP4 expression was detected in immature outer pillar cells (arrow), Hensen's cells, some GER cells, and outer sulcus cells. (D) At P0, AQP4 was expressed in inner sulcus cells, Hensen's cells, Claudius cells, and outer sulcus cells. (E) At E96, FGFR3 expression was detected in hair cells and some SOX2-positive cells. (F, G) At E101 and E115, FGFR3 expression was detected in outer hair cells and some SOX2-positive supporting cells. No expression was detected in inner hair cells. (H) At P0, FGFR3 expression was not detected. (I, J) No CD44 expression was detected at E96 and E101. (K) At E115, CD44 was expressed in both inner and outer pillar cells, and some Claudius cells and Hensen's cell. (L) At P0, CD44 expression was only detected in inner sulcus cells and SOX2-negative Hensen's cells. The nuclei were counterstained with Hoechst (blue). Scale bar: 50 μm. A, B, D, E, G, H, and I: basal turn; C, F, J, K, and L: middle turn. IHC: inner hair cells, OHC, outer hair cells; IPC, inner pillar cells; OPC, outer pillar cells; HC, Hensen's cells. E96 (n = 5), E101 (n = 4), E115 (n = 4), and P0 (n = 3).

in the lateral half of the cochlear duct, including in SOX2-positive cells other than hair cells at E96 (Fig. 7I). At E101, GATA3 expression was restricted to the ventral side, including SOX2-positive cells other than hair cells (Fig. 7J). At E115, we detected GATA3 between Claudius cells and interdental cells. Notably, at this stage, we observed GATA3 expression in outer and inner hair cells (Fig. 7K). At P0, expression was lost from a portion of supporting cells, as reported in mice; however, unlike in mice, GATA3 expression was lost from inner pillar cells, inner pharyngeal cells, and inner border cells but remained detectable in Deiters'

Fig. 9. Developmental changes in the expression patterns of SOX genes. (A, B) At E96 and E101, SOX21 was expressed within the modiolar half of the cochlear duct but not in the spiral ganglion. (C) At E115, SOX21 was expressed in Deiters' cells, inner and outer pillar cells, inner border cells, inner pharyngeal cells, inner sulcus cells, and interdental cells. Expression of SOX2 but not SOX21 was detected in Hensen's cells (arrow in C). (D) At P0, SOX21 was expressed in Hensen's cells, Deiters' cells, inner and outer pillar cells, inner border cells, and inner pharyngeal cells. (E–H) SOX9 was broadly expressed in the sensory epithelium of the developing cochlea during development, except in hair cells. (I–L) SOX10 was broadly expressed in the sensory epithelium of the developing cochlea and spiral ganglion during development, except in hair cells. Scale bar: 50 μm. A–C and E–L: basal turn; D: middle turn. IHC, inner hair cells; OHC, outer hair cells; SGN, spiral ganglion neurons. E96 (n = 5), E101 (n = 4), E115 (n = 4), and P0 (n = 3).

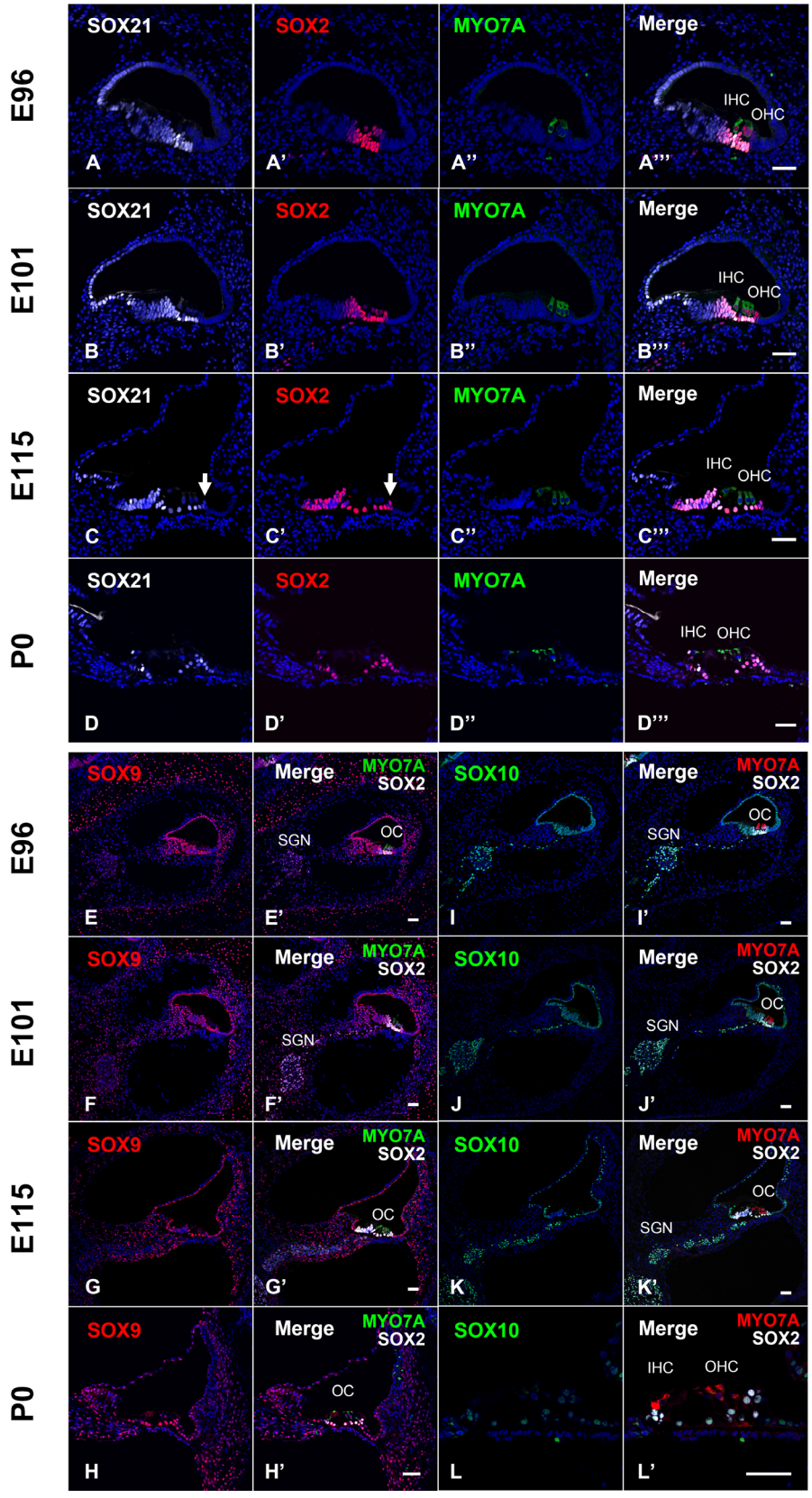
E96
E101
E115
P0
SOX21
SOX2
MYO7A
Merge
IHC
OHC
A
A'
A''
A'''
B
B'
B''
B'''
C
C'
C''
C'''
D
D'
D''
D'''
SOX9
SOX10
MYO7A
SOX2
SGN
OC
E
E'
F
F'
G
G'
H
H'
I
I'
J
J'
K
K'
L
L'

cells, outer pillar cells, Hensen's cells, and Claudius cells in the common marmoset (Figs 5 and 7L).

AQP4, a rapid and highly selective water channel, is thought to facilitate K+ buffering by short-circuiting the accompanying osmotic gradient in the inner ear. In the common marmoset, at E96, we detected AQP4 at the LER and GER. We did not detect expression in hair cells or substantial expression in the sensory epithelium between inner hair cells and outer hair cells (Fig. 8A). At E101, we observed AQP4 in some supporting cells (Fig. 8B). At E115, AQP4 was expressed in immature outer pillar cells, Hensen's cells, inner border cells, inner sulcus cells, and outer sulcus cells (Fig. 8C). At P0, AQP4 was expressed in inner sulcus cells, Hensen's cells, Claudius cells, and outer sulcus cells (Fig. 8D). AQP4 expression was reported in the inner sulcus cells, Hensen's cells, and outer sulcus cells in adult rodents and humans [64-67]. These expression patterns are highly conserved among these species. At birth, in the cochlea of the common marmoset cochlea, we also detected AQP4 expression in these cells (Fig. 8D). Notably, we detected transient expression in outer pillar cells at E115 just before tunnel of Corti formation (Figs 5 and 8C).

Fgfr3 is a key factor in the regulation of pillar cell development and is necessary for the development of the tunnel of Corti [68] in the mouse inner ear. It is thought to function via its principal ligand, FGF8, in the developing cochlea. In mice, Fgfr3 is expressed in inner and outer pillar cells and Deiters' cells from E15.5 to P0. At P7, Fgfr3 expression is maintained in the pillar cells but is absent from Deiters' cells [69,70]. In the common marmoset, we detected FGFR3 expression in both hair cells and a portion of SOX2-positive cells at E96 (Fig. 8E). We also detected expression in inner and outer pillar cells, Deiters' cells, and some Hensen's cells at E101 (Fig. 8F). Its expression was decreased in inner pillar cells, and it was only detected in outer pillar cells, Deiters' cells, and a portion of Hensen's cells at E115 (Fig. 8G). At E101 and E115, we detected FGFR3 in outer hair cells and a portion of SOX2-positive supporting cells. No expression was detected in inner hair cells. At birth, FGFR3 expression was completely lost from the organ of Corti (Figs 5 and 8H).

CD44 is an outer pillar cell marker in the developing mouse cochlea [71]. In mice, by E16, CD44 is expressed in the epithelium of the cochlear duct medially in the regions of the GER and laterally in the area of Claudius cells. CD44 is not expressed in hair cells, pillar cells, Deiters' cells, or Hensen's cells at E16. At P0, CD44 is expressed in the outer pillar cells. After birth, by P24, the expression of CD44 is abolished from the outer pillar cells but persists in the epithelial cells flanking the organ of Corti. In the common marmoset, we first detected CD44 at E115 in both inner and outer pillar cells and a portion of Hensen's cells (Fig. 8I–K). At birth, we did not detect CD44 in pillar cells but observed it in inner sulcus cells and SOX2-negative Hensen's cells flanking the organ of Corti (Figs 5 and 8L).

SOX gene expression during the development of the primate cochlea

Next, we investigated expression patterns of SOX gene family members. SOX genes are important for inner ear development and morphogenesis [72-75]. They are sensory epithelium and/or supporting cell markers in cochlear development. *Sox2* is a member of the SOX B gene family, which includes the SOX B1 subgroup (*Sox1*, *Sox2*, and *Sox3*) and SOX B2 subgroup (*Sox14* and *Sox21*). *Sox2* and *Sox21* have key functions in normal cochlear development in mice [73,76]. We observed that SOX2 expression is highly similar during the development of rodents and the common marmoset, except for its expression along the developing neurites (Figs 5 and 9A–D).

In the common marmoset, we found that SOX21 (SRY-box transcription factor 21) is more broadly expressed than SOX2 in the sensory epithelium of the developing cochlea at E96, and SOX21 is not expressed in hair cells. At E96, SOX21 was expressed in supporting cells surrounding hair cells and within the modiolar half of the cochlear duct, including the developing Reissner's membrane, but was not expressed in the spiral ganglion (Fig. 9A). As development progressed, SOX21 expression in the Reissner's membrane decreased (Fig. 9A–C). At E115, SOX21 was expressed in Deiters' cells, inner and outer pillar cells, inner border cells, inner pharyngeal cells, inner sulcus cells, and interdental cells (Fig. 9C). Notably, in this period, we detected SOX2 but not SOX21 in Hensen's cells, similar to P0 mice (arrow in Fig. 9C) [76]. At P0, SOX21 was expressed in Hensen's cells, Deiters' cells, inner and outer pillar cells, inner border cells, and inner pharyngeal cells (Figs 5 and 9D).

Sox9 (SRY-box transcription factor 9) is a member of the SOX E gene family, which includes *Sox8*, *Sox9*, and *Sox10*. Mutations in *SOX9* in humans result in skeletal abnormalities, XY sex reversal syndrome, and campomelic dysplasia [77]. While this syndrome has a high mortality rate, surviving patients exhibit sensorineural hearing loss, suggesting that SOX9 is involved in inner ear development. In mice, Sox9 is expressed from the time of otocyst formation. At E14.5 and E16.5, Sox9 is expressed in the periotic

mesenchyme, spiral ganglion neurons, and most of the otic epithelium, except in hair cells [74], and its expression overlaps with Sox2 in supporting cells. A similar expression pattern is observed at E18.5. In mice, at E16.5, Sox10 (SRY-box transcription factor 10) is not expressed in hair cells but is continuously expressed in other cochlear duct epithelial cells, and Sox10-positive cells are also observed in the stria vascularis [78]. At P1, Sox10 expression is observed in the spiral ganglion neuron, stria vascularis, GER, LER, and supporting cells but not in hair cells. At P21, Sox10 is expressed in the cochlear epithelium, stria vascularis, Reissner's membrane, and auditory nerve fiber but not in hair cells and tympanic border cells.

The downregulation of SOX9 and SOX10 coincides with the first hair cell commitment, followed by the downregulation of SOX2 several weeks later. Finally, at 19 weeks of gestation, all inner hair cells and outer hair cells are negative for SOX2, SOX9, and SOX10 [38]. In human fetuses, from 10.4 to 19 weeks of gestation, SOX9 is expressed in the periotic mesenchyme, spiral ganglion neuron, and most of the otic epithelium, except in hair cells.

In the common marmoset, SOX9 was broadly expressed in the sensory epithelium of the developing cochlea throughout development, except in hair cells. We also observed broad SOX9 expression in some surrounding periotic mesenchymal cells (Fig. 9E–H). We observed broad SOX10 expression in the sensory epithelium of the developing cochlea and spiral ganglion, except in hair cells. We also detected SOX10 expression in melanocytes migrating to the stria vascularis. Consistent with patterns in mice and humans, the downregulation of SOX9 and SOX10 coincided with the first hair cell commitment, followed by the downregulation of SOX2 (Fig. 9I–L).

Development of spiral ganglion neurons

Next, we examined the development of spiral ganglion neurons in the common marmoset cochlea. Fundamentally, postmitotic neurons of the spiral ganglion extend a single peripheral process toward epithelial target cells long before they differentiate into hair cells. In rodents, initial afferent innervation in the basal region of the cochlea is visible at E12.5 followed by appearance of differentiating hair cells at E14.5 [54,79]. In humans, neurite innervation has been observed at 10 weeks of gestation followed by hair cell differentiation at around 12 weeks [38]. In mice at E13.5, the spiral ganglion neuron is completely peripherin-negative. At E15.5, before Myosin7a expression in outer hair cells, innervation by β-III tubulin-positive neurites to single-row inner hair cells is clearly detected in the basal turn, but innervation by peripherin-positive neurites is not observed. After that, the number of synaptic contacts in the hair cells increases as development progresses and excessive synapses come to be observed around the first postnatal week [80,81]. However, during the following second postnatal week, these immature synapses are either consolidated or removed. Finally, half of the synapses need to be dispelled [82]. This synaptic pruning is related to neurite refinement and the retraction of immature branched spiral ganglion neurons as well as neuronal apoptosis [83,84]. After the removal of immature synapses, mature innervation of type II spiral ganglion neurons to outer hair cells is completed [83,85-88].

Initial neuronal innervation of the cochlear duct is not conserved between mice and humans. Unlike in mice, expression of PRPH (peripherin) is observed at 10 weeks of gestation in spiral ganglion neurons prior to their innervations into hair cells in human. At 12 weeks of gestation, connections between PRPH (peripherin) and TUBB (Tubulin beta, β-III Tubulin) double-positive neurons and inner hair cells are observed. At 14 weeks, connections between these neurons and outer hair cells are observed [38,89]. Extensive PRPH expression has been maintained between 12 and 15 weeks of gestation in neurites reaching both the inner hair cells and outer hair cells. After that, PRPH expression gradually becomes restricted to type II spiral ganglion neurons, with pruning of these neurons by 18–20 weeks of gestation [38]. Unlike in mice or other rodents, this specialization occurs during embryonic period in human.

In the common marmoset cochlea, we observed TUBB and NEFH (neurofilament heavy, NF200)-positive nerve fiber innervation of inner hair cells and outer hair cells at E96 (Fig. 10). PRPH and CALB1 were expressed in the spiral ganglion neuron and NEFH-positive neurofilaments at E96 (Figs 10–12). PRPH and TUBB-positive neurofilaments were directed to the MYO7A-negative prosensory region in the apical turn, as well as to MYO7A-positive inner hair cells and outer hair cells in the middle or basal turns (Fig. 10). These expression patterns in neurites were also detected at E101 and E115 (Figs 11 and 12). The greatest numbers of neuronal projections and neuronal contacts to hair cells were observed at E115 (Figs 11D and 12D,I). At P0, in the common marmoset, neuronal pruning occurred and there were fewer neuronal projections and contacts compared with E115 (Figs 11E and 12E,J). At this point, PRPH expression was restricted to type II neurites directed to outer hair cells. No PRPH expression was detected in neurites near inner hair cells at P0 (Figs 12E and 13).

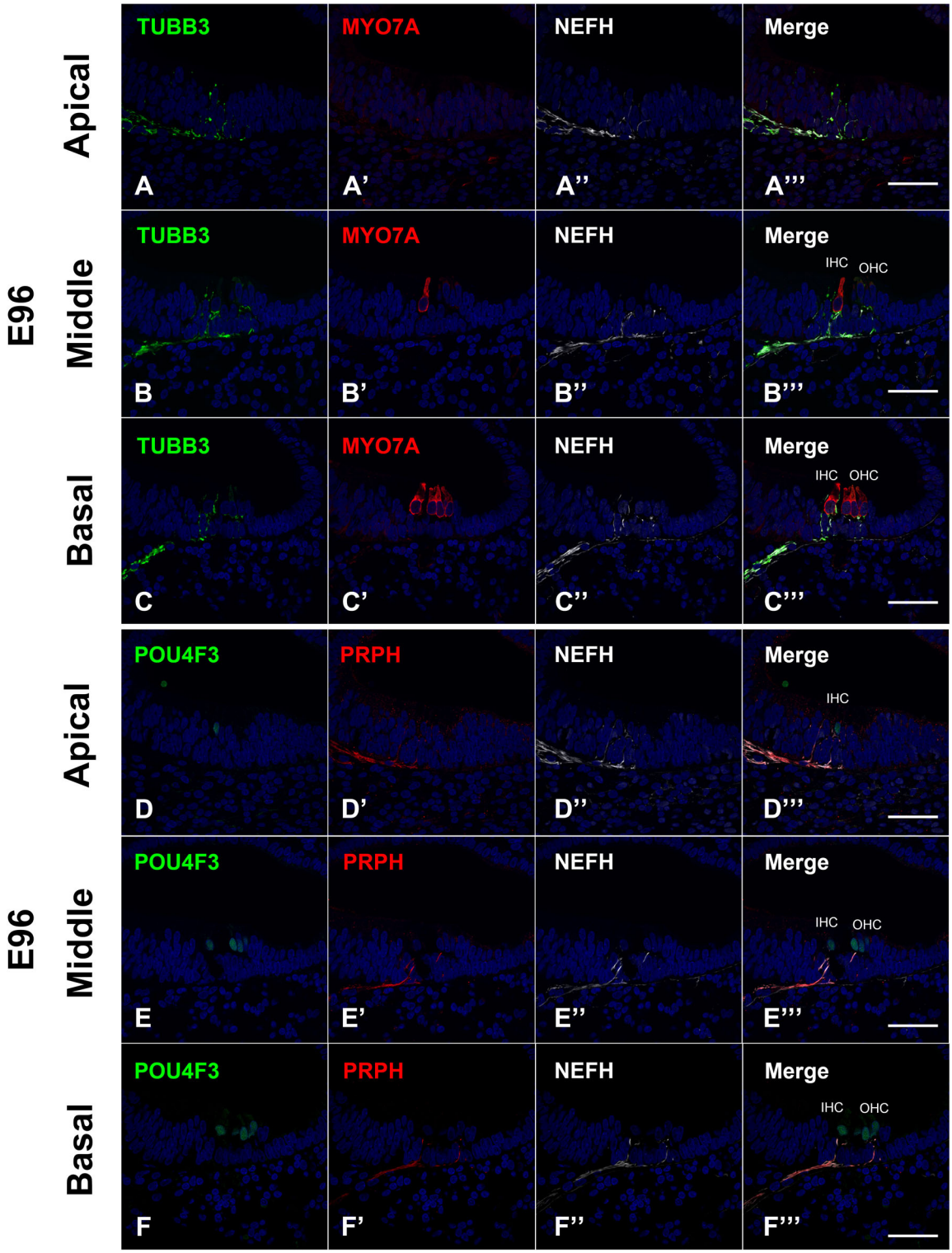

Fig. 10. Early innervation of spiral ganglion neurons into the premature sensory epithelium. (A–F) At E96, TUBB-, PRPH-, and NEFH-positive neuronal fiber innervations were observed. Notably, in the apical turn, where MYO7A was not expressed, neuronal innervation began. Neuronal innervation was more frequent in the basal turn than in the apical turn. The nuclei were counterstained with Hoechst (blue). Scale bar: 50 μm. IHC, inner hair cells; OHC, outer hair cells. E96 (n = 5).

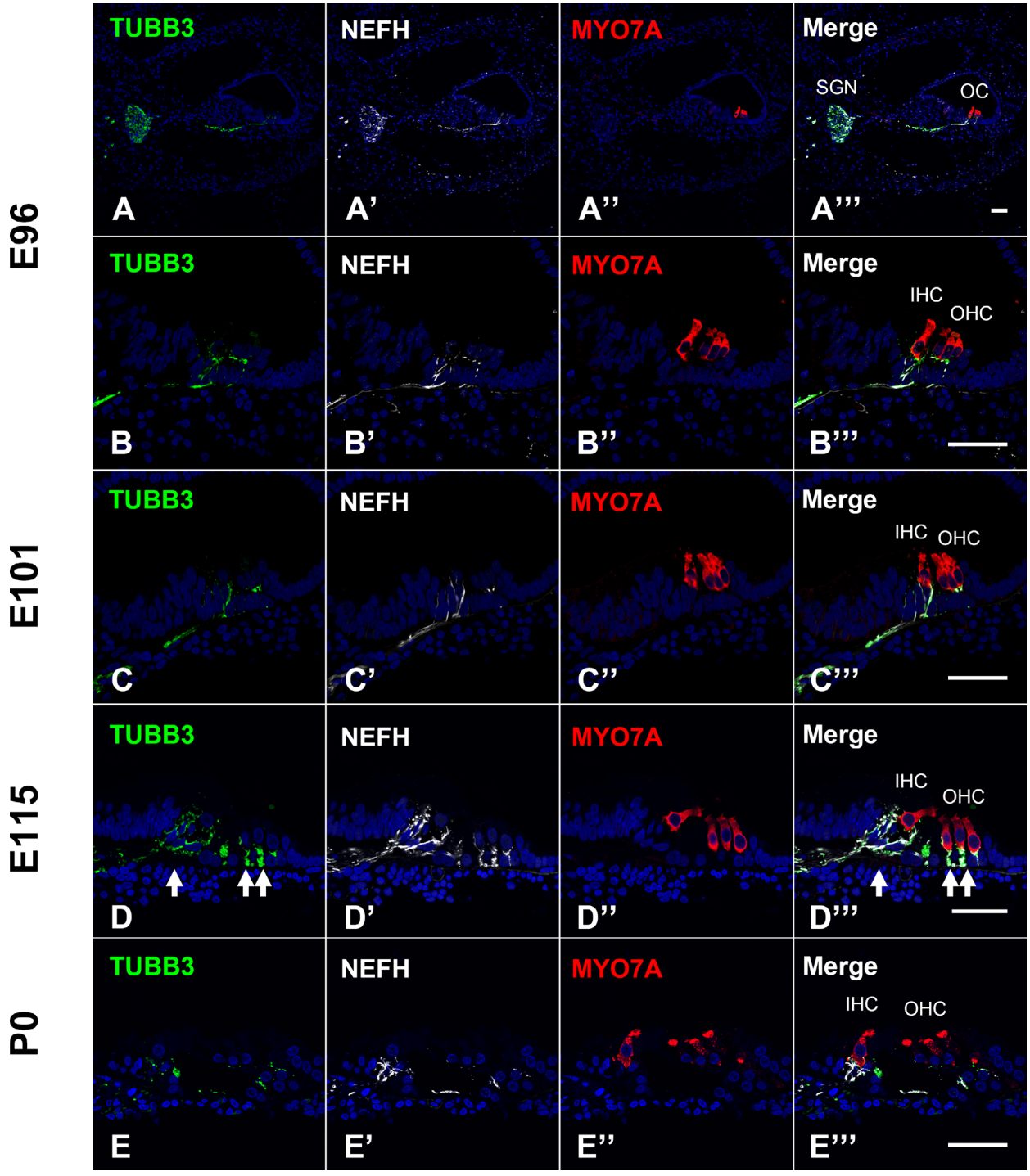

Fig. 11. Development of spiral ganglion neuron of common marmoset. (A, B) At E96-, TUBB-, and NEFH-positive nerve fiber innervations of inner hair cells and outer hair cells were observed at E96. (C, D) After E96, increases in innervating neurites were observed, with the most prominent neuronal contact to both hair cells at E115 (arrow in D). (E) At P0, in the common marmoset, neuronal pruning occurred, and fewer neuronal projections and contacts were observed. The nuclei were counterstained with Hoechst (blue). Scale bar: 50 μm. A: basal turn; B–D: middle turn. IHC, inner hair cells; OHC, outer hair cells. E96 (n = 5), E101 (n = 4), E115 (n = 4), and P0 (n = 3).

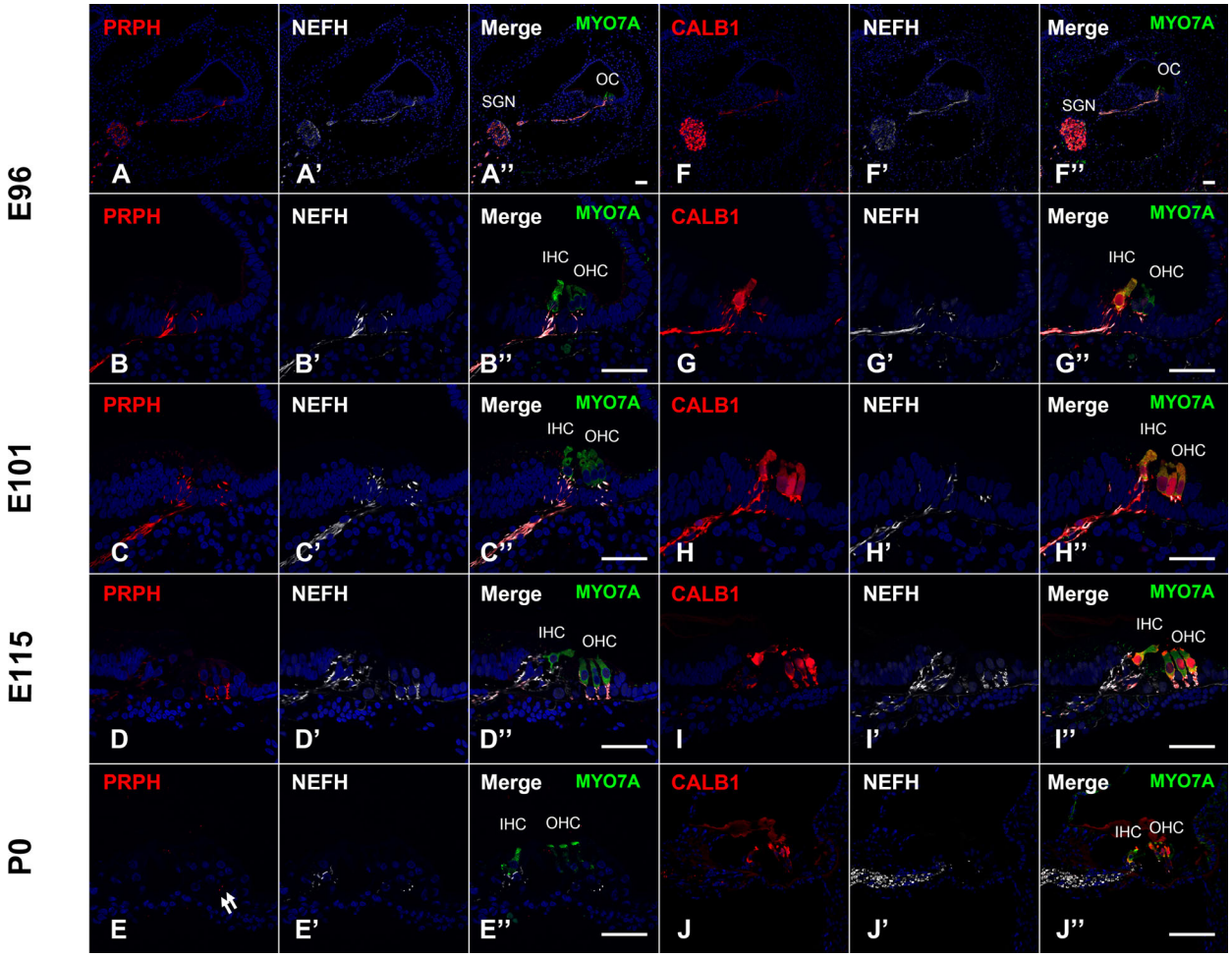

Fig. 12. Changes in the expression patterns of neuronal markers during development. (A, B (Higher magnification of A), F, G (Higher magnification of F)). (A, F) PRPH and CALB1 were expressed in the spiral ganglion neuron and NEFH-positive neurofilaments at E96. PRPH- and CALB1-positive neurofilaments directed to MYO7A-positive inner hair cells and outer hair cells. (C, D, H, and I) Innervations of PRPH- and CALB1-positive neurofilaments to both inner hair cells and outer hair cells were observed in E101 and E115, with decreased expression in neurites at E115. Notably, PRPH expression of type I neurite was decreased. (E, J) At P0, PRPH expression was restricted to the neurons directed to outer hair cells (arrow in E), while CARBINDIN expression was observed in neurons directed to both inner hair cells and outer hair cells. The nuclei were counterstained with Hoechst (blue). Scale bar: 50 μm; A, B, F, and J: basal turn; C–E, H, and I: middle turn. IHC, inner hair cells; OHC, outer hair cells; SGN, spiral ganglion neurons. E96 (n = 5), E101 (n = 4), E115 (n = 4), and P0 (n = 3).

We also found that the expression patterns of neuronal markers in immature neurites in the common marmoset are more similar to those of humans than to those of mice. In the development of afferent innervation of spiral ganglion neurons toward inner hair cells and outer hair cells, a multi-step process is required for neuronal specification and subsequent development toward terminal identity. In rodents and humans, neurite outgrowth and extension toward the sensory epithelium do not require mature targeted hair cells [38,79]. However, PRPH expression differed between rodents and humans. In the common marmoset, we observed neurite outgrowth before hair cell differentiation at E96, and these neurites showed a pattern similar to that in humans, in which PRPH is expressed at this early neuronal innervation stage [38] (Fig. 13).

Several molecular guidance factors that attract or repel outgrowing neurites of spiral ganglion neurons have been identified, including semaphorins and their neuropilin receptors and plexin coreceptors, slit and robo receptors, and netrin-1 and its receptors [90-92]. These molecules are necessary for the formation of an appropriate neurite connection between both type I neurons to inner hair cells and type II neurons to outer hair cells. Moreover, in mice, pillar cells also influence the segregation of spiral ganglion neurons. In

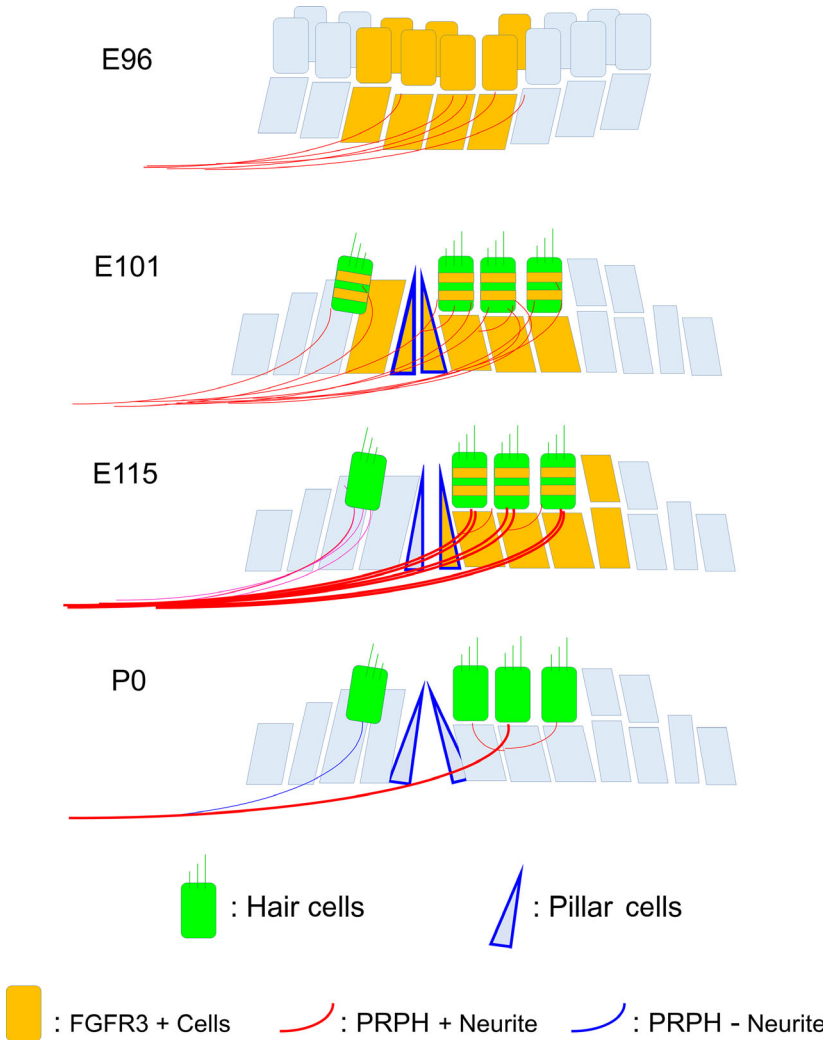

Fig. 13. Schematic diagram of neurite development in the common marmoset. Changes in neuronal marker expression patterns are shown, especially in terms of the relationship between FGFR3 expression. FGFR3-positive cells are indicated in yellow. Peripherin-positive neurite is labeled in red, and peripherin-negative neurite is labeled in blue. Pillar cells are shown by blue frame triangles.

Fgfr3 knockout mice, in which pillar cells are lost, an increased number of neurite fibers cross the pillar cell space to contact outer hair cells [93]. Irrespective of whether this regulation is directly or indirectly dependent on Fgfr3, pillar cells are an important boundary for appropriate neurite specification. In the common marmoset, we found that the expression of FGFR3 itself was not restricted to pillar cells (Fig. 13). This supports the notion that pillar cells, and not FGFR3 expression itself, control type I and type II neurite specification. Further studies are required to improve our understanding of the mechanism by which pillar cells regulate the projection of two distinct neurites.

Development of the stria vascularis and lateral wall fibrocytes

Next, we used immunostaining to detect several stria vascularis-related markers, including NKCC1 (Na-K-Cl cotransporter 1), ATP1A1 (ATPase Na+/K+ transporting subunit alpha 1, Na-K-ATPase α1), and MLANA (Melan A), as well as the fibrocyte markers POU3F4 (POU class 3 homeobox 4), TBX18 (T-box transcription factor 18), and CALD1 (Caldesmon 1) in common marmoset fetuses.

In humans, the first signs of stria vascularis differentiation appear by 11 weeks of gestation, followed by rapid development. At the end of the 13 weeks, morphological signs of functional maturation are observed. The stria vascularis has a layered epithelial structure composed of the three cell types of the lateral wall of the cochlear duct. In humans, the marginal cells lining the cochlear duct are the first cells to develop and are present by 11–12 weeks of gestation. This is followed closely by the appearance of distinct intermediate cells within the epithelium by 12–13 weeks of gestation [94]. Basal cells do not emerge as a distinct epithelial layer until 18 weeks of gestation or later. By 20 weeks of

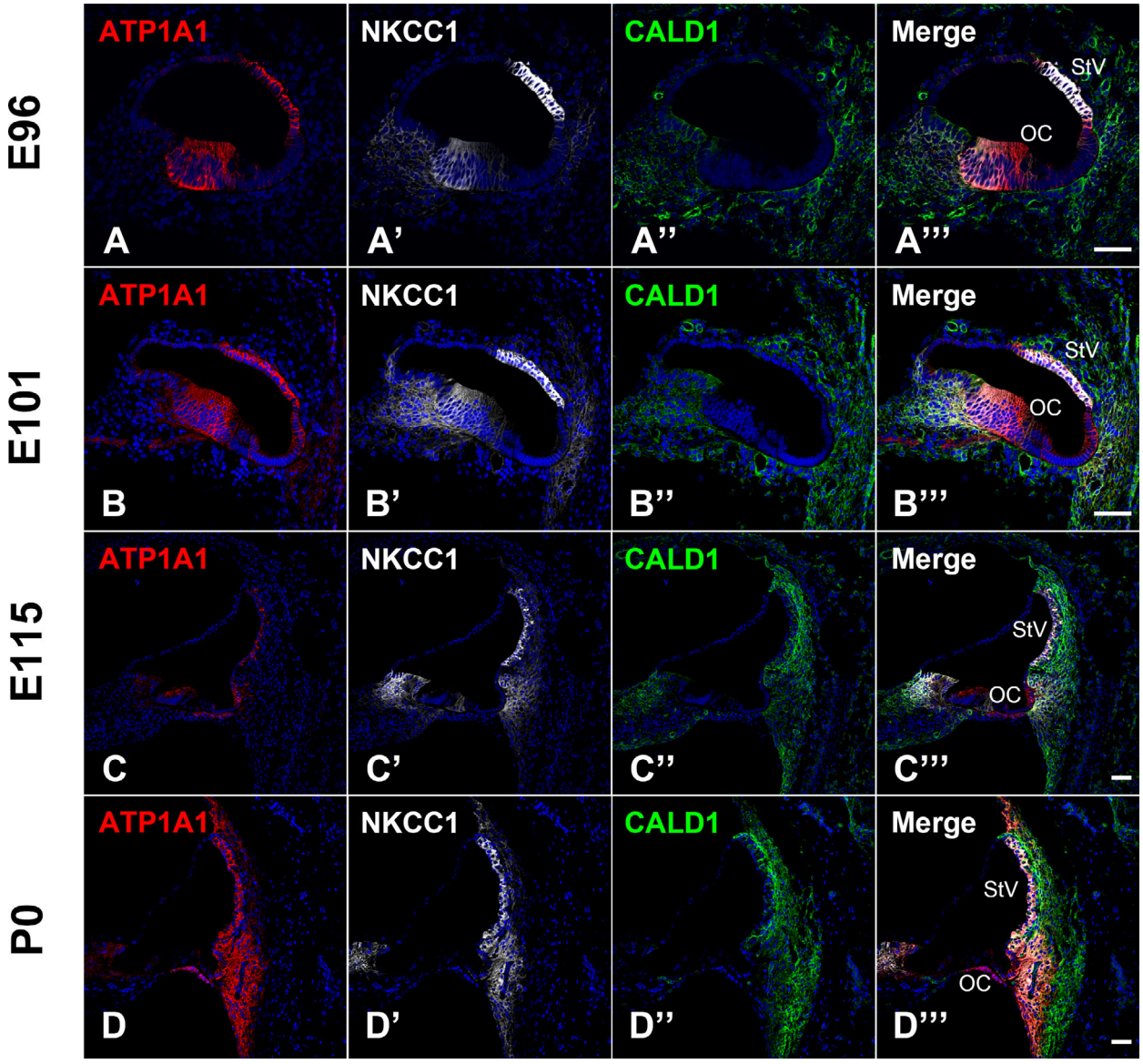

Fig. 14. Development of the stria vascularis in the common marmoset. (A) At E96, NKCC1 and ATP1A1 were expressed in the presumed stria vascularis region on the upper lateral side of the cochlear duct. CALD1 was abundantly expressed in surrounding periotic mesenchymal cells. Their expression was also observed in a part of the sensory epithelium at this stage. (B, C) NKCC1 and ATP1A1 were also expressed in a portion of lateral wall fibrocytes. (D) At P0, NKCC1 immunoreactivity was observed in type II, IV, and V fibrocytes, marginal cells, and spiral limbus cells. ATP1A1 immunoreactivity was observed in type II, IV, and V fibrocytes and marginal cells. CALD1 expression was restricted to type I and type III lateral wall fibrocytes and the spiral limbus. The nuclei were counterstained with Hoechst (blue). Scale bar: 50 μm. A–D: basal turn. OC, organ of Corti; StV, stria vascularis. E96 (n = 5), E101 (n = 4), E115 (n = 4), and P0 (n = 3).

gestation, the stria vascularis attains an adult-like appearance.

NKCC1 and ATP1A1 are key molecules in the potassium recycling pathway of the cochlea. In rodents, humans, and common marmosets, NKCC1 is expressed in lateral wall fibrocytes, marginal cells of the stria vascularis, and spiral limbus cells in adults [28,95,96]. ATP1A1 expression has also been detected in lateral wall fibrocytes and marginal cells of stria vascularis. In adults, the expression patterns of NKCC1 and ATP1A1 are shared between rodents and primates.

In the common marmoset, at E96, the formation of the stria vascularis was not obvious, but NKCC1 and ATP1A1 were detected in the assumed stria vascularis

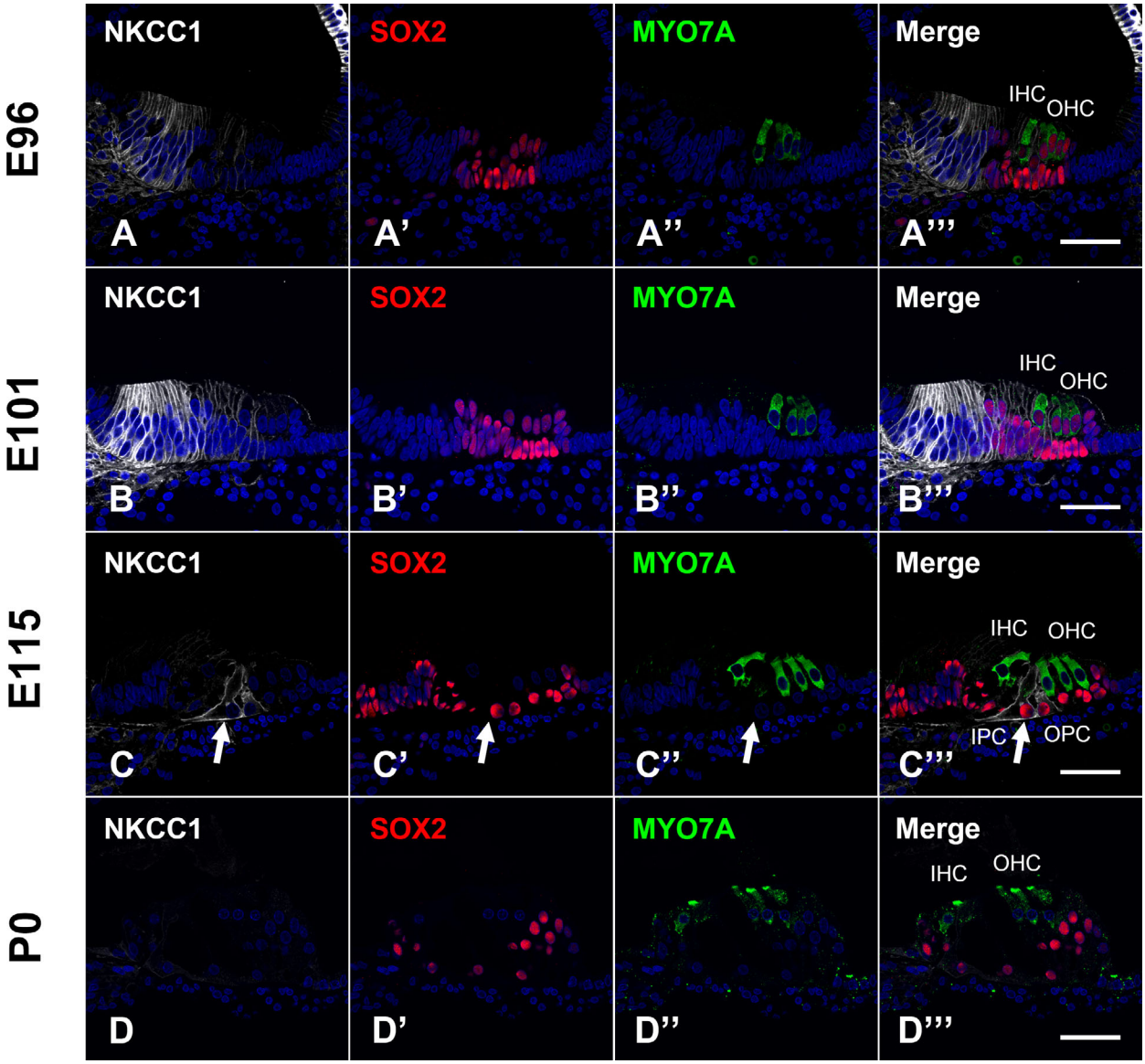

Fig. 15. Changes in expression patterns of NKCC1 in the organ of Corti during development. NKCC1 was transiently expressed in the sensory epithelium. (A, B) At E96 and E101, NKCC1 was expressed in GER and some SOX2-positive supporting cells but not in outer and inner hair cells. (C) At E115, NKCC1 expression was restricted to outer and inner pillar cells (arrow). (D) At P0, NKCC1 was not expressed in the organ of Corti. The nuclei were counterstained with Hoechst (blue). Scale bar: 50 μm. A: basal turn; B–D: middle turn. IHC, inner hair cells; OHC, outer hair cells; IPC, inner pillar cells; OPC, outer pillar cells. E96 (n = 5), E101 (n = 4), E115 (n = 4), and P0 (n = 3).

region on the upper lateral side of the cochlear duct (Fig. 14A). NKCC1 was transiently expressed in sensory epithelial cells (Fig. 15A). At E101, NKCC1 expression was detected at the GER and in a portion of SOX2-positive supporting cells, while no expression was observed in outer or inner hair cells (Fig. 15B). At E115, NKCC1 expression was restricted to outer and inner pillar cells (Fig. 15C). MLANA-positive cells, corresponding to migrating melanocytes or intermediate cells [97], were also observed next to these NKCC1-positive cells (Fig. 16E–H).

The expression of CALD1, a fibrocyte marker [28,98], was abundant in surrounding periotic mesenchymal cells at E96 (Fig. 14A). We also detected its expression in part of the sensory epithelium at this stage. At P0, CALD1 expression was restricted to type I and type III lateral wall fibrocytes and the spiral limbus (Fig. 14D).

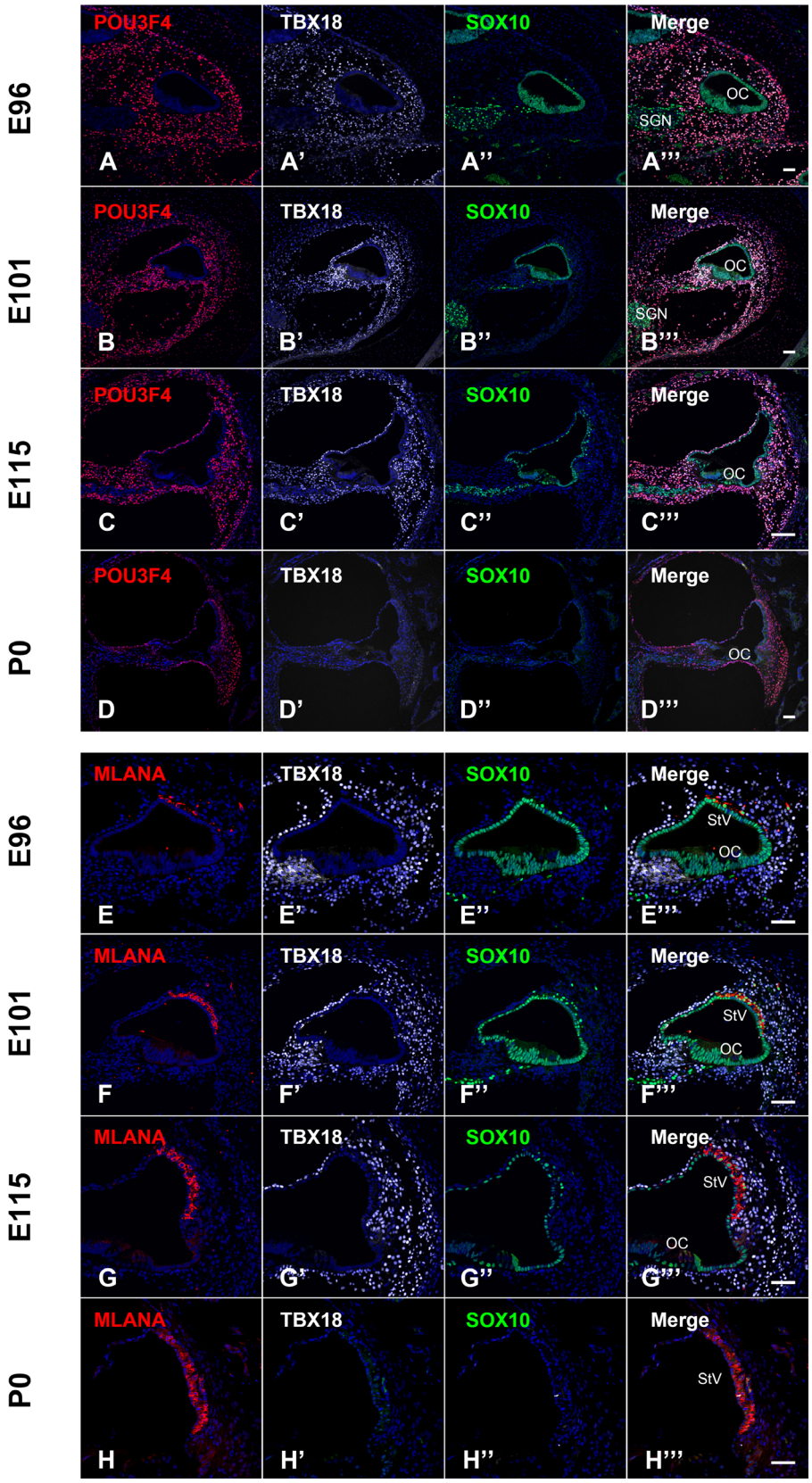
E96
E101
E115
P0
POU3F4
TBX18
SOX10
Merge
OC
SGN
A
A'
A''
A'''
B
B'
B''
B'''
C
C'
C''
C'''
D
D'
D''
D'''
MLANA
StV
E
E'
E''
E'''
F
F'
F''
F'''
G
G'
G''
G'''
H
H'
H''
H'''

Fig. 16. Development of the cochlear lateral wall in the common marmoset. (A–C) POU3F4 and TBX18 were abundantly expressed in surrounding periotic mesenchymal cells at E96, E101, and E115. No expression was detected in SOX10-labeled epithelial cells. (D) At P0, POU3F4 was expressed in the lateral wall fibrocytes, part of Reissner's membrane, spiral limbus, and tympanic border cells, while TBX18 was not expressed in the cochlea. (E–H) MLANA was expressed in migrating cells directed to the stria vascularis at E96 and in the developing intermediate cells of the stria vascularis. The nuclei were counterstained with Hoechst (blue). Scale bar: 50 μm; B–F: basal turn; A, G, and H: middle turn. OC, organ of Corti; StV, stria vascularis; SGN, spiral ganglion neurons. E96 (n = 5), E101 (n = 4), E115 (n = 4), and P0 (n = 3).

POU3F4 and TBX18, which are periotic mesenchymal cell markers [99,100], were highly expressed in surrounding periotic mesenchymal cells at E96, E101, and E115 in the common marmoset (Fig. 16A–C). No expression was detected in SOX10-labeled epithelial cells. At P0, POU3F4 was expressed in the lateral wall fibrocytes, a part of Reissner's membrane, spiral limbus, and tympanic border cells, while no TBX18 expression was detected in the cochlea (Fig. 16D). The expression of conventional markers of the stria vascularis and lateral walls was generally conserved among these three species.

Differences in the time course of cochlear developmental between species

We identified novel transient expression patterns of genes as well as differences in the expression patterns of several genes between rodents and common marmoset. The duration of cochlear development in humans and common marmosets was about 10 weeks, compared with about 3 weeks in mice. Accordingly, studies of the common marmoset may be useful for the detection of transient gene expression, which could be observed over very short time periods. The long duration of development enables us to examine temporal changes in cochlear development at high resolution. For example, we noticed that some stria vascularis markers with transient expression in the organ of Corti have not been reported in the mouse model (Fig. 15). In addition, we observed neuronal projections and pruning for longer periods than those in mice. In the common marmoset, neuronal projections to hair cells were most prominent at E115, and pruning occurred at P0 (Figs 11–13). In mice, neuronal pruning occurred between P6 and P12. Thus, in the common marmoset, neuronal pruning was five times slower than that in the mouse model. Observations of this period might be useful for studies of primate-specific mechanisms of pruning of neurites because it is very difficult to obtain human fetal samples for this period (equivalent to mid-term or late-term abortion). Our results suggested that this model animal is suitable for precise observations of cochlear development and could lead to new findings that cannot be observed in a mouse model.

Usefulness of the common marmoset as a primate cochlear development model

Cochlear development includes a complex series of steps, including prosensory epithelial cell fate decision to either a hair cell or supporting cell fate, spiral ganglion neuron innervation, and cochlear lateral wall formation. In this study, we clearly delineated cochlear development in a nonhuman primate model animal, the common marmoset, including the development of hair cells, spiral ganglion neurons, supporting cells, and the lateral wall, which we believe will be useful for future studies into primate cochlear development and for the development of regenerative or stem cell-based therapies for hearing disorders.

Hearing impairment is the most common symptom of congenital defects and is a major disability in the elderly, including presbycusis. Hearing impairment due to auditory hair cell loss is normally irreversible because mammalian hair cells do not regenerate spontaneously. Thus, hair cell regeneration is an important strategy for the treatment of permanent hearing loss. There are several studies of regenerative therapy for hearing, including cell therapy or drug treatment.

In regenerative therapy, an understanding of organ development and tissue generation is important because re-tracing developmental steps is a promising approach. Moreover, pluripotent stem cell-based cell therapy is expected to be a feasible method for the replacement of damaged cells with new targeted cells induced from pluripotent stem cells, including embryonic stem cells or induced pluripotent stem cells. Detailed developmental information about the target organ or cell type is required for efficient induction of well-differentiated cells.

In this report, we observed similarities as well as differences in cochlear development between the common marmoset, human, and mouse. The expression of conventional markers of hair cells was generally conserved among these three species. Sox gene expression patterns were highly similar. The most prominent differences among species were expression patterns of supporting cell markers. We analyzed ten supporting cell markers (i.e., CDKN1B, SOX2, SOX21, SOX9, SOX10, ISLET1, GATA3, AQP4, FGFR3, and

CD44). The expression patterns of CDKN1B, GATA3, and ISLET1 were clearly different from those of mice. Taken together, the results suggest that several characteristics of supporting cells differ between rodents and primates, although more detailed analyses will be required to identify precisely the differences.

Methods for the regeneration of hair cells have been developed in rodent models [60,101,102]. However, it is not clear whether these methods are applicable to humans or primates. The expression of some targeted genes differs between rodents and primates, including several genes in supporting cells. Notably, we observed that the expression patterns of CDKN1B, GATA3, and ISLET1 clearly differ between rodents and primates. These three genes have been identified as therapeutic targets for hair cell regeneration or hair cell protection [60,61]. Accordingly, primate-specific developmental studies aimed at efficient induction methods from pluripotent stem cells to sensory domains, including hair cells and supporting cells, are needed.

The data reported in this study could also form the basis of future gene modification studies designed to understand cochlear development or disease in primate model animals. The common marmoset is a primate model with established gene modification methods [34-35,103], although gene modification in this species is still limited compared with transgenic mouse models. However, several studies used a transgenic common marmoset model to uncover novel mechanisms underlying human diseases that cannot be reproduced by rodent models [36,104,105]. Our results improve our understanding of inner ear development in the common marmoset, providing a basis for time- or cell type-specific transgenic models (e.g., Cre–loxP-mediated transgenic marmosets) for further studies, and our detailed expression analyses will be useful for controlling Cre expression. For example, POU4F3-mediated conditional control of targeted genes is expected to function similarly in the common marmoset and mouse, whereas GATA3- or CDKN1B-mediated conditional control is expected to be different, based on the distinct expression patterns of these genes in various species.

Human fetal samples are a powerful tool for studying primate-specific cochlear development but are

Table 1. Antibodies used in this study.

Antibody	Host	Isotype	Catalog ID	Provider	Dilution
anti-POU4F3	Mouse	IgG	sc-81980	Santa Cruz Biotechnology, Santa Cruz, CA, USA	1 : 200
anti-PCNA	Rabbit	IgG	PC474	Oncogene, Cambridge, MA, USA	1 : 200
anti-SOX2	Rabbit	IgG	AB92494	Abcam, Cambridge, UK	1 : 200
anti-SOX2	Rat	IgG2A	14-9811-82	Invitrogen, Carlsbad, CA, USA	1 : 200
anti-SOX2	Goat	IgG	AF2018	R&D, Minneapolis, MN, USA	1 : 200
anti-MYOSIN7a	Mouse	IgG	138-1-s	DSHB, Iowa City, IA, USA	1 : 30
anti-MYOSIN7a	Rabbit	IgG	25-6790	Proteus Biosciences, Ramona, CA, USA	1 : 100
anti-SLC26A5	Goat	IgG	sc-22694	Santa Cruz Biotechnology, Santa Cruz, CA, USA	1 : 100
anti-CALB1	Rabbit	IgG	ab11426	Abcam, Cambridge, UK	1 : 1000
anti-CALB2	Rabbit	IgG	GTX103261	GeneTex, Irvine, CA, USA	1 : 200
anti-PVALB	Rabbit	IgG	AB11427	Abcam, Cambridge, UK	1 : 500
anti-CDKN1B	Mouse	IgG	610242	BD, Franklin Lakes, NJ, USA	1 : 200
anti-GATA3	Rabbit	IgG	HPA029731	Atlas Antibodies, Bromma, Sweden	1 : 100
anti-FGFR3	Mouse	IgG	sc-13121	Santa Cruz Biotechnology, Santa Cruz, CA, USA	1 : 50
anti-AQP4	Rabbit	IgG	SC20812	Santa Cruz Biotechnology, Santa Cruz, CA, USA	1 : 400
anti-ISLET1	Rabbit	IgG	ab109517	Abcam, Cambridge, UK	1 : 300
anti-CD44	Rabbit	IgG	AB157107	Abcam, Cambridge, UK	1 : 1000
anti-SOX9	Rabbit	IgG	AB5535	Merck Millipore, Burlington, MA, USA	1 : 100
anti-SOX10	Mouse	IgG	sc-365682	Santa Cruz Biotechnology, Santa Cruz, CA, USA	1 : 100
anti-SOX21	Goat	IgG	AF3538	R&D, Minneapolis, MN, USA	1 : 100
anti-TUBB	Mouse	IgG	GTX631836	GeneTex, Irvine, CA, USA	1 : 1000
anti-NEFH	Chick	IgY	ab4680	Abcam, Cambridge, UK	1 : 1000
anti-PRPH	Rabbit	IgG	AB1530	Merck Millipore, Burlington, MA, USA	1 : 100
anti-NKCC1	Goat	IgG	sc-21545	Santa Cruz Biotechnology, Santa Cruz, CA, USA	1 : 300
anti-ATP1A1	Rabbit	IgG	sc-28800	Santa Cruz Biotechnology, Santa Cruz, CA, USA	1 : 50
anti-MLANA	Rabbit	IgG	NBP1-30151	Novus, St. Charles, MO, USA	1 : 200
anti-POU3F4	Rabbit	IgG	HPA031984	Atlas Antibodies, Bromma, Sweden	1 : 200
anti-TBX18	Goat	IgG	sc-17869	Santa Cruz Biotechnology, Santa Cruz, CA, USA	1 : 50
anti-CALD1	Mouse	IgG	MS-1251-P0	Thermo Fisher Scientific, Waltham, MA, USA	1 : 200

extremely rare, especially for late developmental stages. Thus, our new developmental data provide an effective tool for studying primate cochlear development.

Materials and methods

Specimens

Cadaverous fixed head samples of common marmosets at E96 ($n = 5$), E101 ($n = 4$), E115 ($n = 4$), and P0 ($n = 3$) were kindly provided by Ayako Murayama and the Central Institute for Experimental Animals (CIEA).

The animal experiments were approved by the animal experiment committee of Keio University (number: 11006) and RIKEN (H30-2-214(3)) and were conducted in accordance with the guidelines of the National Institutes of Health and the Ministry of Education, Culture, Sports, Science and Technology of Japan.

Tissue preparation

The temporal bone region of each common marmoset embryo was dissected and fixed with 4% paraformaldehyde in PBS overnight immediately after euthanasia. P0 specimens were decalcified in Decalcifying Solution B (Wako, Osaka, Japan) for 1 week and then embedded in Tissue-Tek O.C.T. compound for cross-sectioning. Seven-micrometer sections were used for immunohistochemistry.

Immunohistochemistry

After a brief wash with PBS, sections were heated (80 °C) in 10 μM citrate buffer (pH 6) for 15 min. After another brief wash, the sections were preblocked for 1 h at room temperature in 10% normal serum in PBS, incubated with primary antibodies at 4 °C overnight, and then incubated with Alexa Fluor-conjugated secondary antibodies for 60 min at room temperature. The nuclei were counterstained with Hoechst 33258.

Antibodies

The primary antibodies used in this study are listed in Table 1. The following secondary antibodies were used: Goat anti-Rabbit IgG, Alexa Fluor Plus 555 (A32732, 1 : 500; Invitrogen), Goat anti-Mouse IgG, Alexa Fluor Plus 488 (A32723, 1 : 500; Invitrogen), Goat anti-Chicken IgY, Alexa Fluor Plus 647 (A21449, 1 : 500; Invitrogen), Goat anti-Rat IgG, Alexa Fluor 647 (ab 150159, 1 : 500; Abcam), Donkey anti-Rabbit IgG, Alexa Fluor 555 (ab 150074, 1 : 500; Abcam), Donkey anti-Mouse IgG, Alexa Fluor 488 (ab 150105, 1 : 500; Abcam), and Donkey anti-Goat IgG, Alexa Fluor 647 (705-605-147, 1 : 500; Jackson Immuno-Research, West Grove, PA, USA).

Acknowledgements

We thank Ayano Mitsui, Saki Ninomiya, and Junko Okahara for technical support and Takeshi Inoue for providing materials. MH was supported by a grant from the Japanese government MEXT KAKENHI (Grant-in-Aid for Early-Career Scientists, 18K16856), the Keio Medical Association and Keio University Medical Science Fund, the Society for Promotion of International Oto-Rhino-Laryngology (SPIO), and Keio Gijuku Academic Development Funds. This research was also partially supported by grants to MF from the Japanese government MEXT KAKENHI (Grant-in-Aid for Scientific Research (A) 18H04065, 19H05473), Keio Gijuku Academic Development Funds, foundation from Mitsubishi Tanabe, and the Takeda Science Foundation. This research was also partially supported by a Grant for Brain Mapping by Integrated Neurotechnologies for Disease Studies (Brain/MINDS).

Conflict of interest

HO is a founding scientist and a paid Scientific Advisory Board Member of San Bio Co., Ltd. MH, MF, and KO are founding scientists of Otolink Co., Ltd.

Author contributions

MH, MF, AYM, HO, and KO conceived and designed the experiments. MH and MF wrote the manuscript. MH performed most of the experiments and analyzed the data. All authors read and approved the final version of the manuscript.

References

1 Basch ML, Brown RM II, Jen HI & Groves AK (2016) Where hearing starts: the development of the mammalian cochlea. *J Anat* **228**, 233–254.
2 Schulz-Mirbach T, Ladich F, Plath M & Hess M (2019) Enigmatic ear stones: what we know about the functional role and evolution of fish otoliths. *Biol Rev Camb Philos Soc* **94**, 457–482.
3 Wilczynski W & Capranica RR (1984) The auditory system of anuran amphibians. *Prog Neurogibol* **22**, 1–38.
4 Manley GA (2002) Evolution of structure and function of the hearing organ of lizards. *J Neurobiol* **53**, 202–211.
5 Manley GA (2011) Lizard auditory papillae: an evolutionary kaleidoscope. *Hear Res* **273**, 59–64.
6 Koppl C (2011) Birds–same thing, but different? Convergent evolution in the avian and mammalian

auditory systems provides informative comparative models. *Hear Res* **273**, 65–71.
7 Fritzsch B & Elliott KL (2017) Gene, cell, and organ multiplication drives inner ear evolution. *Dev Biol* **431**, 3–15.
8 Nothwang HG (2016) Evolution of mammalian sound localization circuits: a developmental perspective. *Prog Neurogibol* **141**, 1–24.
9 Ekdale EG (2013) Comparative anatomy of the bony labyrinth (inner ear) of placental mammals. *PLoS ONE* **8**, e66624.
10 Ladhams A & Pickles JO (1996) Morphology of the monotreme organ of Corti and macula lagena. *J Comp Neurol* **366**, 335–347.
11 Schultz JA, Zeller U & Luo ZX (2017) Inner ear labyrinth anatomy of monotremes and implications for mammalian inner ear evolution. *J Morphol* **278**, 236–263.
12 Ekdale EG (2016) Form and function of the mammalian inner ear. *J Anat* **228**, 324–337.
13 Ruf I, Luo ZX, Wible JR & Martin T (2009) Petrosal anatomy and inner ear structures of the Late Jurassic Henkelotherium (Mammalia, Cladotheria, Dryolestoidea): insight into the early evolution of the ear region in cladotherian mammals. *J Anat* **214**, 679–693.
14 Luo ZX, Ruf I, Schultz JA & Martin T (2011) Fossil evidence on evolution of inner ear cochlea in Jurassic mammals. *Proc Biol Sci* **278**, 28–34.
15 Bryant J, Goodyear RJ & Richardson GP (2002) Sensory organ development in the inner ear: molecular and cellular mechanisms. *Br Med Bull* **63**, 39–57.
16 Wu DK & Kelley MW (2012) Molecular mechanisms of inner ear development. *Cold Spring Harb Perspect Biol* **4**, a008409.
17 Barald KF & Kelley MW (2004) From placode to polarization: new tunes in inner ear development. *Development* **131**, 4119–4130.
18 Groves AK & Fekete DM (2012) Shaping sound in space: the regulation of inner ear patterning. *Development* **139**, 245–257.
19 Avraham KB (2003) Mouse models for deafness: lessons for the human inner ear and hearing loss. *Ear Hear* **24**, 332–341.
20 Friedman LM, Dror AA & Avraham KB (2007) Mouse models to study inner ear development and hereditary hearing loss. *Int J Dev Biol* **51**, 609–631.
21 Armstrong SD, Bloch JI, Houde P & Silcox MT (2011) Cochlear labyrinth volume in euarchontoglirans: implications for the evolution of hearing in primates. *Anat Rec (Hoboken)* **294**, 263–266.
22 Gultekin YB & Hage SR (2017) Limiting parental feedback disrupts vocal development in marmoset monkeys. *Nat Commun* **8**, 14046.
23 Eliades SJ & Miller CT (2017) Marmoset vocal communication: behavior and neurobiology. *Dev Neurobiol* **77**, 286–299.
24 Wang X & Kadia SC (2001) Differential representation of species-specific primate vocalizations in the auditory cortices of marmoset and cat. *J Neurophysiol* **86**, 2616–2620.
25 Osmanski MS, Song X & Wang X (2013) The role of harmonic resolvability in pitch perception in a vocal nonhuman primate, the common marmoset (*Callithrix jacchus*). *J Neurosci* **33**, 9161–9168.
26 Johnson LA, Della Santina CC & Wang X (2012) Temporal bone characterization and cochlear implant feasibility in the common marmoset (*Callithrix jacchus*). *Hear Res* **290**, 37–44.
27 Johnson LA, Della Santina CC & Wang X (2016) Selective neuronal activation by cochlear implant stimulation in auditory cortex of awake primate. *J Neurosci* **36**, 12468–12484.
28 Hosoya M, Fujioka M, Ogawa K & Okano H (2016) Distinct expression patterns of causative genes responsible for hereditary progressive hearing loss in non-human primate cochlea. *Sci Rep* **6**, 22250.
29 Hosoya M, Fujioka M, Okano H & Ogawa K (2016) Distinct expression pattern of a deafness gene, KIAA1199, in a primate cochlea. *Biomed Res Int* **2016**, 1–8.
30 Suzuki N, Hosoya M, Oishi N, Okano H, Fujioka M & Ogawa K (2016) Expression pattern of wolframin, the WFS1 (Wolfram syndrome-1 gene) product, in common marmoset (*Callithrix jacchus*) cochlea. *Neuroreport* **27**, 833–836.
31 Matsuzaki S, Hosoya M, Okano H, Fujioka M & Ogawa K (2018) Expression pattern of EYA4 in the common marmoset (*Callithrix jacchus*) cochlea. *Neurosci Lett* **662**, 185–188.
32 Saeki T, Hosoya M, Shibata S, Okano H, Fujioka M & Ogawa K (2019) Distribution of tight junctions in the primate cochlear lateral wall. *Neurosci Lett* **717**, 134686.
33 Hosoya M, Fujioka M, Kobayashi R, Okano H & Ogawa K (2016) Overlapping expression of anion exchangers in the cochlea of a non-human primate suggests functional compensation. *Neurosci Res* **110**, 1–10.
34 Sasaki E, Suemizu H, Shimada A, Hanazawa K, Oiwa R, Kamioka M, Tomioka I, Sotomaru Y, Hirakawa R, Eto T *et al.* (2009) Generation of transgenic non-human primates with germline transmission. *Nature* **459**, 523–527.
35 Sato K, Oiwa R, Kumita W, Henry R, Sakuma T, Ito R, Nozu R, Inoue T, Katano I, Sato K *et al.* (2016) Generation of a nonhuman primate model of severe combined immunodeficiency using highly efficient genome editing. *Cell Stem Cell* **19**, 127–138.

36 Park JE, Zhang XF, Choi SH, Okahara J, Sasaki E & Silva AC (2016) Generation of transgenic marmosets expressing genetically encoded calcium indicators. *Sci Rep* **6**, 34931.
37 Hall JW III (2000) Development of the ear and hearing. *J Perinatol* **20**, S12–S20.
38 Locher H, Frijns JH, van Iperen L, de Groot JC, Huisman MA, de Sousa Chuva & Lopes SM (2013) Neurosensory development and cell fate determination in the human cochlea. *Neural Dev* **8**, 20.
39 Hearn JP, Lunn SF, Burden FJ & Pilcher MM (1975) Management of marmosets for biomedical research. *Lab Anim* **9**, 125–134.
40 Kim JH, Rodriguez-Vazquez JF, Verdugo-Lopez S, Cho KH, Murakami G & Cho BH (2011) Early fetal development of the human cochlea. *Anat Rec (Hoboken)* **294**, 996–1002.
41 Xiang MQ, Maklad A, Pirvola U & Fritzsch B (2003) Brn3c null mutant mice show long-term, incomplete retention of some afferent inner ear innervation. *BMC Neurosci* **4**, 2.
42 Hasson T, Heintzelman MB, Santos-Sacchi J, Corey DP & Mooseker MS (1995) Expression in cochlea and retina of myosin VIIa, the gene product defective in Usher syndrome type 1B. *Proc Natl Acad Sci USA* **92**, 9815–9819.
43 Dechesne CJ & Thomasset M (1988) Calbindin (CaBP 28 kDa) appearance and distribution during development of the mouse inner ear. *Brain Res* **468**, 233–242.
44 Adler HJ, Belyantseva IA, Merritt RC, Frolenkov GI, Dougherty GW & Kachar B (2003) Expression of prestin, a membrane motor protein, in the mammalian auditory and vestibular periphery. *Hear Res* **184**, 27–40.
45 Dechesne CJ, Rabejac D & Desmadryl G (1994) Development of calretinin immunoreactivity in the mouse inner ear. *J Comp Neurol* **346**, 517–529.
46 Heller S, Bell AM, Denis CS, Choe Y & Hudspeth AJ (2002) Parvalbumin 3 is an abundant Ca2+ buffer in hair cells. *J Assoc Res Otolaryngol* **3**, 488–498.
47 Vahava O, Morell R, Lynch ED, Weiss S, Kagan ME, Ahituv N, Morrow JE, Lee MK, Skvorak AB, Morton CC *et al.* (1998) Mutation in transcription factor POU4F3 associated with inherited progressive hearing loss in humans. *Science* **279**, 1950–1954.
48 Xiang M, Gao WQ, Hasson T & Shin JJ (1998) Requirement for Brn-3c in maturation and survival, but not in fate determination of inner ear hair cells. *Development* **125**, 3935–3946.
49 Masuda M, Dulon D, Pak K, Mullen LM, Li Y, Erkman L & Ryan AF (2011) Regulation of POU4F3 gene expression in hair cells by 5' DNA in mice. *Neuroscience* **197**, 48–64.
50 Gibson F, Walsh J, Mburu P, Varela A, Brown KA, Antonio M, Beisel KW, Steel KP & Brown SD (1995) A type VII myosin encoded by the mouse deafness gene shaker-1. *Nature* **374**, 62–64.
51 Self T, Mahony M, Fleming J, Walsh J, Brown SD & Steel KP (1998) Shaker-1 mutations reveal roles for myosin VIIA in both development and function of cochlear hair cells. *Development* **125**, 557–566.
52 Weil D, Kussel P, Blanchard S, Levy G, Levi-Acobas F, Drira M, Ayadi H & Petit C (1997) The autosomal recessive isolated deafness, DFNB2, and the Usher 1B syndrome are allelic defects of the myosin-VIIA gene. *Nat Genet* **16**, 191–193.
53 Liu XZ, Walsh J, Mburu P, Kendrick-Jones J, Cope MJ, Steel KP & Brown SD (1997) Mutations in the myosin VIIA gene cause non-syndromic recessive deafness. *Nat Genet* **16**, 188–190.
54 Chen P & Segil N (1999) p27(Kip1) links cell proliferation to morphogenesis in the developing organ of Corti. *Development* **126**, 1581–1590.
55 Abe T, Kakehata S, Kitani R, Maruya S, Navaratnam D, Santos-Sacchi J & Shinkawa H (2007) Developmental expression of the outer hair cell motor prestin in the mouse. *J Membr Biol* **215**, 49–56.
56 Simmons DD, Tong B, Schrader AD & Hornak AJ (2010) Oncomodulin identifies different hair cell types in the mammalian inner ear. *J Comp Neurol* **518**, 3785–3802.
57 Li C, Shu Y, Wang G, Zhang H, Lu Y, Li X, Li G, Song L & Liu Z (2018) Characterizing a novel vGlut3-P2A-iCreER knockin mouse strain in cochlea. *Hear Res* **364**, 12–24.
58 Wan G, Corfas G & Stone JS (2013) Inner ear supporting cells: rethinking the silent majority. *Semin Cell Dev Biol* **24**, 448–459.
59 Lowenheim H, Furness DN, Kil J, Zinn C, Gultig K, Fero ML, Frost D, Gummer AW, Roberts JM, Rubel EW *et al.* (1999) Gene disruption of p27(Kip1) allows cell proliferation in the postnatal and adult organ of Corti. *Proc Natl Acad Sci USA* **96**, 4084–4088.
60 Walters BJ, Coak E, Dearman J, Bailey G, Yamashita T, Kuo B & Zuo J (2017) In vivo interplay between p27(Kip1), GATA3, ATOH1, and POU4F3 converts non-sensory cells to hair cells in adult mice. *Cell Rep* **19**, 307–320.
61 Huang M, Kantardzhieva A, Scheffer D, Liberman MC & Chen ZY (2013) Hair cell overexpression of Islet1 reduces age-related and noise-induced hearing loss. *J Neurosci* **33**, 15086–15094.
62 Radde-Gallwitz K, Pan L, Gan L, Lin X, Segil N & Chen P (2004) Expression of Islet1 marks the sensory and neuronal lineages in the mammalian inner ear. *J Comp Neurol* **477**, 412–421.
63 Luo XJ, Deng M, Xie X, Huang L, Wang H, Jiang L, Liang G, Hu F, Tieu R, Chen R *et al.* (2013) GATA3 controls the specification of prosensory domain and

neuronal survival in the mouse cochlea. *Hum Mol Genet* **22**, 3609–3623.
64 Takumi Y, Nagelhus EA, Eidet J, Matsubara A, Usami S, Shinkawa H, Nielsen S & Ottersen OP (1998) Select types of supporting cell in the inner ear express aquaporin-4 water channel protein. *Eur J Neurosci* **10**, 3584–3595.
65 Miyabe Y, Kikuchi T & Kobayashi T (2002) Comparative immunohistochemical localizations of aquaporin-1 and aquaporin-4 in the cochleae of three different species of rodents. *Tohoku J Exp Med* **196**, 247–257.
66 Lopez IA, Ishiyama G, Lee M, Baloh RW & Ishiyama A (2007) Immunohistochemical localization of aquaporins in the human inner ear. *Cell Tissue Res* **328**, 453–460.
67 Eckhard A, Gleiser C, Rask-Andersen H, Arnold H, Liu W, Mack A, Muller M, Lowenheim H & Hirt B (2012) Co-localisation of K(ir)4.1 and AQP4 in rat and human cochleae reveals a gap in water channel expression at the transduction sites of endocochlear K (+) recycling routes. *Cell Tissue Res* **350**, 27–43.
68 Colvin JS, Bohne BA, Harding GW, McEwen DG & Ornitz DM (1996) Skeletal overgrowth and deafness in mice lacking fibroblast growth factor receptor 3. *Nat Genet* **12**, 390–397.
69 Hayashi T, Cunningham D & Bermingham-McDonogh O (2007) Loss of Fgfr3 leads to excess hair cell development in the mouse organ of Corti. *Dev Dyn* **236**, 525–533.
70 Shim K, Minowada G, Coling DE & Martin GR (2005) Sprouty2, a mouse deafness gene, regulates cell fate decisions in the auditory sensory epithelium by antagonizing FGF signaling. *Dev Cell* **8**, 553–564.
71 Hertzano R, Puligilla C, Chan SL, Timothy C, Depireux DA, Ahmed Z, Wolf J, Eisenman DJ, Friedman TB, Riazuddin S *et al.* (2010) CD44 is a marker for the outer pillar cells in the early postnatal mouse inner ear. *J Assoc Res Otolaryngol* **11**, 407–418.
72 Neves J, Kamaid A, Alsina B & Giraldez F (2007) Differential expression of Sox2 and Sox3 in neuronal and sensory progenitors of the developing inner ear of the chick. *J Comp Neurol* **503**, 487–500.
73 Kiernan AE, Pelling AL, Leung KKH, Tang ASP, Bell DM, Tease C, Lovell-Badge R, Steel KP & Cheah KSE (2005) Sox2 is required for sensory organ development in the mammalian inner ear. *Nature* **434**, 1031–1035.
74 Mak AC, Szeto IY, Fritzsch B & Cheah KS (2009) Differential and overlapping expression pattern of SOX2 and SOX9 in inner ear development. *Gene Expr Patterns* **9**, 444–453.
75 Watanabe K, Takeda K, Katori Y, Ikeda K, Oshima T, Yasumoto K, Saito H, Takasaka T & Shibahara S (2000) Expression of the Sox10 gene during mouse inner ear development. *Brain Res Mol Brain Res* **84**, 141–145.
76 Hosoya M, Fujioka M, Matsuda S, Ohba H, Shibata S, Nakagawa F, Watabe T, Wakabayashi K-I, Saga Y & Ogawa K (2011) Expression and function of Sox21 during mouse cochlea development. *Neurochem Res* **36**, 1261–1269.
77 Wagner T, Wirth J, Meyer J, Zabel B, Held M, Zimmer J, Pasantes J, Bricarelli FD, Keutel J, Hustert E *et al.* (1994) Autosomal sex reversal and campomelic dysplasia are caused by mutations in and around the SRY-related gene SOX9. *Cell* **79**, 1111–1120.
78 Breuskin I, Bodson M, Thelen N, Thiry M, Borgs L, Nguyen L, Lefebvre PP & Malgrange B (2009) Sox10 promotes the survival of cochlear progenitors during the establishment of the organ of Corti. *Dev Biol* **335**, 327–339.
79 Koundakjian EJ, Appler JL & Goodrich LV (2007) Auditory neurons make stereotyped wiring decisions before maturation of their targets. *J Neurosci* **27**, 14078–14088.
80 Roux I, Hosie S, Johnson SL, Bahloul A, Cayet N, Nouaille S, Kros CJ, Petit C & Safieddine S (2009) Myosin VI is required for the proper maturation and function of inner hair cell ribbon synapses. *Hum Mol Genet* **18**, 4615–4628.
81 Huang LC, Barclay M, Lee K, Peter S, Housley GD, Thorne PR & Montgomery JM (2012) Synaptic profiles during neurite extension, refinement and retraction in the developing cochlea. *Neural Dev* **7**, 38.
82 Sendin G, Bulankina AV, Riedel D & Moser T (2007) Maturation of ribbon synapses in hair cells is driven by thyroid hormone. *J Neurosci* **27**, 3163–3173.
83 Wiechers B, Gestwa G, Mack A, Carroll P, Zenner HP & Knipper M (1999) A changing pattern of brain-derived neurotrophic factor expression correlates with the rearrangement of fibers during cochlear development of rats and mice. *J Neurosci* **19**, 3033–3042.
84 Barclay M, Ryan AF & Housley GD (2011) Type I vs type II spiral ganglion neurons exhibit differential survival and neuritogenesis during cochlear development. *Neural Dev* **6**, 33.
85 Echteler SM & Nofsinger YC (2000) Development of ganglion cell topography in the postnatal cochlea. *J Comp Neurol* **425**, 436–446.
86 Rueda J, de la Sen C, Juiz JM & Merchan JA (1987) Neuronal loss in the spiral ganglion of young rats. *Acta Otolaryngol* **104**, 417–421.
87 Defourny J, Poirrier AL, Lallemend F, Mateo Sanchez S, Neef J, Vanderhaeghen P, Soriano E, Peuckert C, Kullander K, Fritzsch B *et al.* (2013) Ephrin-A5/EphA4 signalling controls specific afferent targeting to cochlear hair cells. *Nat Commun* **4**, 1438.
88 Delacroix L & Malgrange B (2015) Cochlear afferent innervation development. *Hear Res* **330**, 157–169.

89 Pechriggl EJ, Bitsche M, Glueckert R, Rask-Andersen H, Blumer MJ, Schrott-Fischer A & Fritsch H (2015) Development of the innervation of the human inner ear. *Dev Neurobiol* **75**, 683–702.
90 Miyazaki N, Furuyama T, Takeda N, Inoue T, Kubo T & Inagaki S (1999) Expression of mouse semaphorin H mRNA in the inner ear of mouse fetuses. *Neurosci Lett* **261**, 127–129.
91 Yuan WL, Zhou LJ, Chen TH, Wu JY, Rao Y & Ornitz DM (1999) The mouse SLIT family: secreted ligands for ROBO expressed in patterns that suggest a role in morphogenesis and axon guidance. *Dev Biol* **212**, 290–306.
92 Abraira VE, Del Rio T, Tucker AF, Slonimsky J, Keirnes HL & Goodrich LV (2008) Cross-repressive interactions between Lrig3 and netrin 1 shape the architecture of the inner ear. *Development* **135**, 4091–4099.
93 Puligilla C, Feng F, Ishikawa K, Bertuzzi S, Dabdoub A, Griffith AJ, Fritzsch B & Kelley MW (2007) Disruption of fibroblast growth factor receptor 3 signaling results in defects in cellular differentiation, neuronal patterning, and hearing impairment. *Dev Dyn* **236**, 1905–1917.
94 Lavigne-Rebillard M & Bagger-Sjoback D (1992) Development of the human stria vascularis. *Hear Res* **64**, 39–51.
95 Weber PC, Cunningham CD 3rd & Schulte BA (2001) Potassium recycling pathways in the human cochlea. *Laryngoscope* **111**, 1156–1165.
96 Crouch JJ, Sakaguchi N, Lytle C & Schulte BA (1997) Immunohistochemical localization of the Na-K-Cl co-transporter (NKCC1) in the gerbil inner ear. *J Histochem Cytochem* **45**, 773–778.
97 Locher H, de Groot JC, van Iperen L, Huisman MA, Frijns JH, de Sousa Chuva & Lopes SM (2015) Development of the stria vascularis and potassium regulation in the human fetal cochlea: insights into hereditary sensorineural hearing loss. *Dev Neurobiol* **75**, 1219–1240.
98 Suko T, Ichimiya I, Yoshida K, Suzuki M & Mogi G (2000) Classification and culture of spiral ligament fibrocytes from mice. *Hear Res* **140**, 137–144.
99 Ahn KJ, Passero F Jr & Crenshaw EB III (2009) Otic mesenchyme expression of Cre recombinase directed by the inner ear enhancer of the Brn4/Pou3f4 gene. *Genesis* **47**, 137–141.
100 Trowe MO, Maier H, Schweizer M & Kispert A (2008) Deafness in mice lacking the T-box transcription factor Tbx18 in otic fibrocytes. *Development* **135**, 1725–1734.
101 Mizutari K, Fujioka M, Hosoya M, Bramhall N, Okano HJ, Okano H & Edge AS (2013) Notch inhibition induces cochlear hair cell regeneration and recovery of hearing after acoustic trauma. *Neuron* **77**, 58–69.
102 McLean WJ, Yin X, Lu L, Lenz DR, McLean D, Langer R, Karp JM & Edge AS (2017) Clonal expansion of Lgr5-positive cells from mammalian cochlea and high-purity generation of sensory hair cells. *Cell Rep* **18**, 1917–1929.
103 Okano H & Kishi N (2018) Investigation of brain science and neurological/psychiatric disorders using genetically modified non-human primates. *Curr Opin Neurobiol* **50**, 1–6.
104 Tomioka I, Nogami N, Nakatani T, Owari K, Fujita N, Motohashi H, Takayama O, Takae K, Nagai Y & Seki K (2017) Generation of transgenic marmosets using a tetracyclin-inducible transgene expression system as a neurodegenerative disease model. *Biol Reprod* **97**, 772–780.
105 Tomioka I, Ishibashi H, Minakawa EN, Motohashi HH, Takayama O, Saito Y, Popiel HA, Puentes S, Owari K, Nakatani T *et al.* (2017) Transgenic monkey model of the polyglutamine diseases recapitulating progressive neurological symptoms. *eNeuro* **4**, 0250-16.